(12) INTERNATIONAL APPLICATION PUBLISHED UNDER THE PATENT COOPERATION TREATY (PCT)

(19) World Intellectual Property Organization
International Bureau

(43) International Publication Date
27 October 2011 (27.10.2011)

PCT

(10) International Publication Number
WO 2011/131671 A1

(51) International Patent Classification:
A61K 47/48 (2006.01) *C07K 14/00* (2006.01)
C07K 14/78 (2006.01) *B82Y 5/00* (2011.01)
C12N 5/00 (2006.01)

(21) International Application Number:
PCT/EP2011/056237

(22) International Filing Date:
19 April 2011 (19.04.2011)

(25) Filing Language: English

(26) Publication Language: English

(30) Priority Data:
PCT/IB2010/051700 19 April 2010 (19.04.2010) IB

(71) Applicant *(for all designated States except US)*: **UNIVERSITA' DEGLI STUDI DI MILANO BICOCCA** [IT/IT]; Piazza dell' Ateneo Nuovo, 1, I-20126 Milano (IT).

(72) Inventors; and

(75) Inventors/Applicants *(for US only)*: **VESCOVI, Angelo Luigi** [IT/CH]; Via al Parco 12, CH-6817 Maroggia (CH). **GELAIN, Fabrizio** [IT/IT]; Via della Resistenza 15, I-20094 Corsico (IT).

(74) Agents: **ZACCARO, Elisabetta** et al.; Corso di Porta Vittoria 9, I-20122 Milano (IT).

(81) Designated States *(unless otherwise indicated, for every kind of national protection available)*: AE, AG, AL, AM, AO, AT, AU, AZ, BA, BB, BG, BH, BR, BW, BY, BZ, CA, CH, CL, CN, CO, CR, CU, CZ, DE, DK, DM, DO, DZ, EC, EE, EG, ES, FI, GB, GD, GE, GH, GM, GT, HN, HR, HU, ID, IL, IN, IS, JP, KE, KG, KM, KN, KP, KR, KZ, LA, LC, LK, LR, LS, LT, LU, LY, MA, MD, ME, MG, MK, MN, MW, MX, MY, MZ, NA, NG, NI, NO, NZ, OM, PE, PG, PH, PL, PT, RO, RS, RU, SC, SD, SE, SG, SK, SL, SM, ST, SV, SY, TH, TJ, TM, TN, TR, TT, TZ, UA, UG, US, UZ, VC, VN, ZA, ZM, ZW.

(84) Designated States *(unless otherwise indicated, for every kind of regional protection available)*: ARIPO (BW, GH, GM, KE, LR, LS, MW, MZ, NA, SD, SL, SZ, TZ, UG, ZM, ZW), Eurasian (AM, AZ, BY, KG, KZ, MD, RU, TJ, TM), European (AL, AT, BE, BG, CH, CY, CZ, DE, DK, EE, ES, FI, FR, GB, GR, HR, HU, IE, IS, IT, LT, LU, LV, MC, MK, MT, NL, NO, PL, PT, RO, RS, SE, SI, SK, SM, TR), OAPI (BF, BJ, CF, CG, CI, CM, GA, GN, GQ, GW, ML, MR, NE, SN, TD, TG).

Declarations under Rule 4.17:

— *of inventorship (Rule 4.17(iv))*

Published:

— *with international search report (Art. 21(3))*

— *before the expiration of the time limit for amending the claims and to be republished in the event of receipt of amendments (Rule 48.2(h))*

— *with sequence listing part of description (Rule 5.2(a))*

(54) Title: NOVEL SELF-ASSEMBLING PEPTIDES AND THEIR USE IN THE FORMATION OF HYDROGELS

(57) Abstract: There is described a group of novel self-assembling peptides (SAPs), comprising biotinylated and unbiotinylated sequences, hybrid peptide-peptoid sequences, branched sequences for a total of 48 tested motifs, showing a heterogeneous ensemble of spontaneously self-assembled structures at the nano- and microscale, ranging from short tabular fibers to twisted ribbons, nanotubes and hierarchical self-assembled micrometer-long sheets. Specifically, the SAPs according to the present invention which initially spontaneous assemble, surprisingly form stable solid scaffolds upon exposure to neutral pH buffer. Further these SAPs allow adhesion, proliferation and differentiaton of murine and human neural stem cells and have self-healing propensity. They also did not exert toxic effects in the central nervous system, can stop bleeding and foster nervous regeneration. Therefore, the SAPs according to the present invention are improved biomaterials, a highly valid and useful alternative which may replace the known SAPs, thus overcoming the disadvantages related thereto.

WO 2011/131671 A1

NOVEL SELF-ASSEMBLING PEPTIDES AND THEIR USE IN THE FORMATION OF HYDROGELS

Field of the invention

The present invention concerns the field of synthetic hydrogels. This polymeric class of materials has a wide range of applications in the biomedical field, in electrochemical biosensing, in self-assembling circuits and transistors for computers and in material sciences due to its high versatility.

State of the art

Hydrogels, mainly ascribable to soft materials, have a wide range of applications in 3-D cell culturing, drug delivery and tissue engineering (1-3). There are numerous examples of synthetic or natural polymer-based hydrogels.

Natural derived polymers, including agarose, collagen, fibrin, chitosan, and hyaluronic acid, can form hydrogels. Despite their origin, natural components have several disadvantages, such as the tendency to induce inflammatory response and pathogen transfer due to undefined factors that cannot be eliminated by purification prior to implantation, the significant degree of variability between different lots and the difficulty of availability of large scale sources, particularly if human proteins are involved.

Synthetic polymers can be of two types, those made of small low molecular weight peptides and those made of large monomers such as poly (ethylene glycol), polyacrylamide, poly (vinyl alcohol). This second class of synthetic polymers can form hydrogels under suitable conditions. However, regardless of their purity of chemical tailorability such synthetic hydrogels made of large monomers have several disadvantages such as: biocompatibility, biodegradation products and host responses upon transplantation. Moreover functionalization with bioactive motifs (from 3 to 8-mer peptides), necessary to obtain the desired cellular response, has can be achieved with usually harsh reactions available only for a limited number of short peptides.

Research related to low molecular weight self-assembling peptides which can form hydrogels, synthetic but naturally inspired, has been rapidly expanding in the recent years.

Construction of self-assembling small molecular hydrogels has received

considerable attention due to their potential as nanostructured materials amenable of easy functionalization and capable of creating microenvironments suited for culturing cells, triggering tissue regeneration and other applications beyond life-sciences such as electorchemical sensing, molecular electronics and construction of three-dimensional nanoscale systems.

Peptide-based scaffolds are interesting candidates for hydrogelation because they can be self-assembled in mild solvent conditions via formation of various non-covalent interactions in water, including hydrogen-bonding, electrostatic, or π-π interactions. These interactions, eventually, lead to the formation of organized supramolecular assemblies that can give rise to nanofibers, nanotubes and nanoparticles (7, 8).

The need is therefore increasingly felt for novel synthetic peptides belonging to the promising class of self-assembling peptides for the development of solid scaffolds, which are synthetic but naturally inspired: both precious qualities that allow for molecular design, safe usage in clinics and reasonable scale up production in clinics. Further, such novel polymers need to overcome the disadvantages described above.

Up to now, the majority of known self-assembling short peptides which form synthetic hydrogels are N-terminally protected.

Few examples of hydrogels formed from self-assembling, water-soluble, synthetic short oligopeptides having no protecting group have been described: among them the most important class comprises peptides of alternating hydrophilic and hydrophobic amino acid residues such as described in US7371719 and in US 6548630 (7).

In fact, US20090162437 provides self-assembling peptides with a first amino acid domain which mediates self-assembly, comprising alternating hydrophobic and hydrophilic amino acids that self-assemble into a macroscopic structure when present in unmodified form; and a second amino acid domain that does not mediate self-assembly in isolated form, wherein the second amino acid domain comprises at least one minimal biologically active sequence.

Several functional motifs have been attached to self-assembling peptides. It is known that that the functional motif, BMHP, a member of the class of bone marrow

homing peptides has the following sequence PFSSTKT (SEQ ID NO. 48), and can foster neural stem cell adhesion and differentiation (5). BMPH can stabilize the β–sheet structures (10) found in the self-assembling peptide RADA16-I nanofibers, when linked, via a glycine-spacer, to the RADA16-I self-assembling "core". Nonetheless most of the known self-assembling peptides feature poor mechanical properties, giving very soft and fragile scaffolds when assembled.

Therefore, it is the object of the present invention to find improved SAPs which overcome the disadvantages related to known SAPs and may replace them.

Summary of the invention

The present invention concerns the self-assembling peptide (SAP) which consists of an amino acid domain, having from 7 to 17aminoacids, said domain being:

-GGGPFSSTKT-	SEQ ID N.1
-WGGGPFSSTKT-	SEQ ID N.2
-GGGPFSSTDT-	SEQ ID N.3
-GGGPFSSTNT-	SEQ ID N.4
-GGGPFSSTET-	SEQ ID N.5
-GGGPFSSTQT-	SEQ ID N.6
-GGGAFSSTKT-	SEQ ID N.7
-GGGPFSETKT-	SEQ ID N.8
-GGGAFSSTKTGRGD-	SEQ ID N.9
-GGGPFSSTRT-	SEQ ID N.10
-GGGAFASTKT-	SEQ ID N.11
-GGGGGPFSSTKT-	SEQ ID N.12
-GGGPWSSTKT-	SEQ ID N.13
-GGG(Propylamine)FSSTKT-	SEQ ID N.14
-WGGGAFASTKT-	SEQ ID N.15
-WGGGAFSSTKT-	SEQ ID N.16
-GGGKFSSTPT-	SEQ ID N.17
-GGGPKSSTFT-	SEQ ID N.18
-GGGPFSSKTT-	SEQ ID N.19
-GGGPFSSTTK-	SEQ ID N.20
-GGGGPFSSTKT-	SEQ ID N.21

-GGGPFSSTKTGRGD-	SEQ ID N.22
-GPFSSTKT-	SEQ ID N.23
-GGGAWASTKT-	SEQ ID N.24
-GGGAFASTKA-	SEQ ID N.25
-GGGPFSSTKTP	SEQ ID N.26
-FGGGPFSSTKT-	SEQ ID N.27
-GGGPYSSTKT-	SEQ ID N.28
-GGGAASSTKT-	SEQ ID N.29
-GGGAFAATKT-	SEQ ID N.30
-GGGAFASAKA-	SEQ ID N.31
-GGGPFSSTAT-	SEQ ID N.32
-GGGAFAAAKA-	SEQ ID N.33
-GGGPFSSAKT-	SEQ ID N.34
-GGGPFSATKT-	SEQ ID N.35
-GGGPFSCTKT-	SEQ ID N.36
-GGGPFCSTKT-	SEQ ID N.37
-GAFASTKT-	SEQ ID N.38
-GGGGGAFASTKT-	SEQ ID N.39
-GGGAFASTKTGRGD-	SEQ ID N.40
-GGGPFSSTKTGIKVAV-	SEQ ID N.41
-GGGAFASTKTGIKVAV-	SEQ ID N.42
-GGGAFAK-	SEQ ID N.43
-$(GGG)_2$-KFSSTKT-	SEQ ID N.44
-FGGGAFASTKTGIKVAV-	SEQ ID N.45
-YGGGPFSSTKT-	SEQ ID N.46; or
-FGGGAFSSTKT-	SEQ ID N.47.

The present invention therefore concerns a novel group of self-assembling peptides (SAPs), wherein the SAPs consist of novel peptides, which are optionally biotinylated and unbiotinylated sequences at the N-termini and amidated or not at the C-termini, hybrid peptide-peptoid sequences, for a total of 47 tested motifs. The SAPs having a sequence from SEQ ID NO 1 to SEQ ID NO 47 are all linear

peptides, with the exception of SEQ ID NO.44 which is a branched peptide with two identical GGG branches.

For the purposes of the present invention, each peptide has a peptide identification number and a corresponding SEQ ID NO., as indicated in the following detailed description.

The present invention further describes a hydrogel comprising the self-assembling peptides and a hydrogelating ingredient.

A further aspect of the present invention is a self-assembling peptide polymer comprising at least 2 identical self-assembling peptides.

A still further aspect of the present invention is a self-assembling peptide polymer comprising at least 2 different self-assembling peptides.

A still further aspect is the use of the self-assembling peptide polymer of the invention as a medicament.

The present invention further describes a tabular nanofiber comprising at least 2 identical self-assembling peptides.

The present invention still further describes a tabular nanofiber comprising at least 2 different self-assembling peptides.

A further aspect of the present invention is a complex interwoven membrane made of at least 2 tabular nanofibres.

A still further aspect of the invention is a self-assembled nanostructure consisting of 2 or more identical peptides of the invention.

A still further aspect of the invention is a self-assembled nanostructure consisting of 2 or more different peptides of the invention.

A still further aspect of the invention is a pharmaceutical composition comprising at least one polymer and a pharmaceutically bioactive excipient.

Brief description of the drawings

The characteristics and advantages of the present invention will be apparent from the detailed description reported below, from the Examples given for illustrative and non-limiting purposes, and from the annexed Figures, wherein:

Figure 1 shows an ‘a priori’ classification of the tested sequences.

Figure 2 shows a gelation experiment of the self-assembling peptides in which solution G’ kinetic dependency on peptide concentration is shown;

Figure (2b): storage modulus (G') of peptide B3 dissolved at 3% concentration reaches a plateau after 2 days (variation of 7% between day 2 and day 5), while G' still importantly increases at day 5 in the case of a 2% solution;

Figure (2c): typical measurements of storage (G') and loss (G'') moduli of assembled scaffolds after pH shift (peptides 4, B15, B22) and as a control the still liquid solution of the non-assembling peptide B7 (Biot-PFSSTKT-$CONH_2$);

Figure (2d) shows identification numbers and the corresponding SEQ ID NO., sequences and average values of the storage moduli, for the tested peptides, of peptide solutions (G' pre-assembling) and jellified scaffolds (G' post-assembling).

* Peptide dissolved and tested at 1%;

"peptide tested 7 days after dissolution;

**peptide dissolved and tested at 3%;

^peptide dissolved and tested at 2%.

Figure 3 shows results of Atomic Force Microscopy imaging of the tested peptides.

Figure 3a) Self-assembling peptides B64, B65, B66 and B67 formed twisted nanofiber formations (60 nm pitch, left-handed) since 1 day post dissolution, and also self-assembled giving a hydrogel upon exposure to PBS.

Figure 3b) Self-assembling peptides B15, B24, B32, B33, B40, B41, B42, B44, B54, B58, 59 and 61 self-assembled into flat tabular fibers;

Figure 3c) Self-assembling peptide 4, 37 and 60 yielded twisted fibers.;

Figure 3d) Self-assembling peptides B10, B11, B12, B13 and B43 are shown and form twisted fibers;

Figure 3e) Self-assembling peptides B18, B19, B25, B28, B29, 30, 31, B45, B52, B51, B53 and B50 are shown and form twisted fibers;

Figure 3f) (i) B3, B17, B22, B27, B34, B39, B46, B47, B48 and B57 hierarchically self-assembled into twisted protofibrils;

Figure 3f) (ii), packed together to give ribbons ;

Figure 3f) (iii), assembled into straight tubular structures;

Figure 3f) (iv) and re-arranged into eventual flat sheets.

Figure 4 (a) shows X-ray diffraction pattern.

Figure 4 (b) radial integrated diffracted intensity recorded for B3 peptide. Most significant peaks are identified at 21 Å and 4.6 Å, presumably indicating self-

assembled fibers thickness and a predominant secondary β-sheet structure respectively. Peak at 5.2 Å can be ascribed at distance between stacked aromatic groups. 3.7 Å peak can be interpreted as chains packing at VDW distance.

Figure 4 (c) intensity peaks are summarized for twelve peptides. The strongest peak is at 4.6 Å while peaks at 3.7 Å and 2.35 Å are shared by all tested peptides.

Figure 4 (d) the CD spectra of peptide B24 showed approximately 35% of random coil and 60% of beta-structures (210-230 nm wavelength region).

Similar results were obtained for the other tested peptides.

Figure 5 shows the results of cell culture experiments are shown. hNSCs were cultured for 7 days in vitro on self-assembled scaffolds from solutions and various peptide concentrations of B3, 4, B15, B17, B19, B22, B24, B25, B27, B28 and 31.

Figure 5 (a) Imaged cell morphologies comprise branched and adhered cells, in case of B24, or single spherical cells, as depicted in 30 and in the negative control (plastic).

Figure 5 (b) Live/dead cell assays showed spherical clusters of living cells in the negative control as well as bipolar cells in B22 and a layer of widely branched cells in B24.

Figure 5 (c) Cell titer assay (n=6) of cells cultured for 7 days over the above mentioned self-assembled scaffolds. Notably, B15 and B24 showed the biggest living cell populations, significantly different from negative control ($P<0.002$ and $P<0.001$ respectively; paired t-test.).

Figure 5 (d) NSCs cultured for 14 DIV over B24 scaffolds show positivity for GFAP (87.72%±0.49%), βIIITubulin (12.27%±0.49%), MAP2 (9.5%±0.1%) and GalC/O4 (1.63%±0.37%) markers (n=4).

Figure 6: Self-healing tests

Figure 6 (a) self-healing tests for peptide B17

Figure 6 (b) self-healing tests for peptide B25

Figure 6 (c) self-healing tests for peptide KLD-12.

Frequency sweeps of assembled scaffold after PBS addition, after rupture and at 30 minutes subsequent time points. In (a) the storage modulus gets back to values similar to those of the assembled scaffold before rupture in 120 minutes, in (c) G' values after rupture are stable. Time sweep test of assembled scaffold of B25 after

addition of PBS (b): G' values after rupture recovered in 100 minutes and steadily plateaued after recovery.

Figure 7: B24 biocompatibility in vivo. First row: animal belonging to control group. Second row: treated animal. The hematoma spontaneously occurring in the spinal cord of saline-injected animals (A) was prevented in animal receiving injections of B24 (F). Hematoxilin-Eosin staining of the injection-site in saline-treated and in B24-treated animals (B and G respectively). In control group and in treated animals we detected similar concentrations of infiltrated macrophages (green cells in C and H respectively), apoptotic cells (green cells in D and I respectively) and degenerating nervous fibers (green cells in E and J respectively). Cell nuclei (blue) are stained with DAPI. Scale bar 100 µm.

Figure 8: B24 assessment of nervous regeneration in vivo: longitudinal sections of the spinal cords. a) nervous fibers stained for βIIITubulin and GAP-43 neuronal markers infiltrated the injected self-assembled scaffold of B24 at 1 months after surgery (asterisks point at the scaffold). b) high-magnified image depicting bundles of regenerating nervous fibers within the implanted scaffold. Cell nuclei are marked with DAPI.

Detailed description of the invention

The self-assembling peptide (SAP) of the present invention consists of an amino acid domain, having from 7 to 17 aminoacids, said domain being:

-GGGPFSSTKT-	SEQ ID N.1
-WGGGPFSSTKT-	SEQ ID N.2
-GGGPFSSTDT-	SEQ ID N.3
-GGGPFSSTNT-	SEQ ID N.4
-GGGPFSSTET-	SEQ ID N.5
-GGGPFSSTQT-	SEQ ID N.6
-GGGAFSSTKT-	SEQ ID N.7
-GGGPFSETKT-	SEQ ID N.8
-GGGAFSSTKTGRGD-	SEQ ID N.9
-GGGPFSSTRT-	SEQ ID N.10
-GGGAFASTKT-	SEQ ID N.11
-GGGGGPFSSTKT-	SEQ ID N.12

-GGGPWSSTKT-	SEQ ID N.13
-GGG(Propylamine)FSSTKT-	SEQ ID N.14
-WGGGAFASTKT-	SEQ ID N.15
-WGGGAFSSTKT-	SEQ ID N.16
-GGGKFSSTPT-	SEQ ID N.17
-GGGPKSSTFT-	SEQ ID N.18
-GGGPFSSKTT-	SEQ ID N.19
-GGGPFSSTTK-	SEQ ID N.20
-GGGGPFSSTKT-	SEQ ID N.21
-GGGPFSSTKTGRGD-	SEQ ID N.22
-GPFSSTKT-	SEQ ID N.23
-GGGAWASTKT-	SEQ ID N.24
-GGGAFASTKA-	SEQ ID N.25
-GGGPFSSTKTP	SEQ ID N.26
-FGGGPFSSTKT-	SEQ ID N.27
-GGGPYSSTKT-	SEQ ID N.28
-GGGAASSTKT-	SEQ ID N.29
-GGGAFAATKT-	SEQ ID N.30
-GGGAFASAKA-	SEQ ID N.31
-GGGPFSSTAT-	SEQ ID N.32
-GGGAFAAAKA-	SEQ ID N.33
-GGGPFSSAKT-	SEQ ID N.34
-GGGPFSATKT-	SEQ ID N.35
-GGGPFSCTKT-	SEQ ID N.36
-GGGPFCSTKT-	SEQ ID N.37
-GAFASTKT-	SEQ ID N.38
-GGGGGAFASTKT-	SEQ ID N.39
-GGGAFASTKTGRGD-	SEQ ID N.40
-GGGPFSSTKTGIKVAV-	SEQ ID N.41
-GGGAFASTKTGIKVAV-	SEQ ID N.42
-GGGAFAK-	SEQ ID N.43
-$(GGG)_2$-KFSSTKT-	SEQ ID N.44

-FGGGAFASTKTGIKVAV- SEQ ID N.45

-YGGGPFSSTKT- SEQ ID N.46; or

-FGGGAFSSTKT- SEQ ID N.47.

As above mentioned, for the purposes of the present invention, each peptide has a peptide number and a corresponding SEQ ID NO., according to the following Table 1:

TABLE 1

Peptide number	SEQ ID NO.	SAP amino acid sequence	derivated SAP amino acid sequence
B3 2	SEQ ID NO. 1	GGGPFSSTKT	Biot-GGGPFSSTKT-CONH2, Ac-GGGPFSSTKT-CONH2
4	SEQ ID NO. 2	WGGGPFSSTKT	Ac-WGGGPFSSTKT-CONH2
B10	SEQ ID NO. 3	GGGPFSSTDT	Biot-GGGPFSSTDT-CONH2
B11	SEQ ID NO.4	GGGPFSSTNT	Biot-GGGPFSSTNT-CONH2
B12	SEQ ID NO.5	GGGPFSSTET	Biot-GGGPFSSTET-CONH2
B13	SEQ ID NO. 6	GGGPFSSTQT	Biot-GGGPFSSTQT-CONH2
B15	SEQ ID NO. 7	GGGAFSSTKT	Biot-GGGAFSSTKT-CONH2
B17	SEQ ID NO. 8	GGGPFSETKT	Biot-GGGPFSETKT-CONH2
B19	SEQ ID NO.9	GGGAFSSTKTGRGD	Biot-GGGAFSSTKTGRGD-CONH2
B22	SEQ ID NO. 10	GGGPFSSTRT	Biot-GGGPFSSTRT-CONH2
B24 B55	SEQ ID NO. 11	GGGAFASTKT	Biot-GGGAFASTKT-CONH2 Biot-GGGAFASTKT-COOH
B25	SEQ ID NO. 12	GGGGGPFSSTKT	Biot-GGGGGPFSSTKT-CONH2
B27	SEQ ID NO.13	GGGPWSSTKT	Biot-GGGPWSSTKT-CONH2
B28	SEQ ID NO.14	GGG(Propylamine)FSSTKT	Biot-GGG(Propylamine)FSSTKT-CONH2
30	SEQ ID NO.15	WGGGAFASTKT	Ac-WGGGAFASTKT-CONH2
31	SEQ ID NO.16	WGGGAFSSTKT	Ac-WGGGAFSSTKT-CONH2
B64	SEQ ID NO.17	GGGKFSSTPT	Biot-GGGKFSSTPT-CONH2
B65	SEQ ID NO.18	GGGPKSSTFT	Biot-GGGPKSSTFT-CONH2
B66	SEQ ID NO.19	GGGPFSSKTT	Biot-GGGPFSSKTT-CONH2
B67	SEQ ID NO.20	GGGPFSSTTK	Biot-GGGPFSSTTK-CONH2
B38	SEQ ID NO. 21	GGGGPFSSTKT	Biot-GGGGPFSSTKT-CONH2
B18	SEQ ID NO.22	GGGPFSSTKTGRGD	Biotin-GGGPFSSTKTGRGD-CONH2
B29	SEQ ID NO.23	GPFSSTKT	Biotin-GPFSSTKT-NH2
B32	SEQ ID NO.24	GGGAWASTKT	Biotin-GGGAWASTKT-NH2

B33	SEQ ID NO.25	GGGAFASTKA	Biotin-GGGAFASTKA-NH2
B34	SEQ ID NO.26	GGGPFSSTKTP	Biotin-GGGPFSSTKTP-NH2
37	SEQ ID NO.27	FGGGPFSSTKT	Ac-FGGG-PFSSTKT-CONH2
B39	SEQ ID NO.28	GGGPYSSTKT	Biotin-GGG-PYSSTKT-CONH2
B40	SEQ ID NO.29	GGGAASSTKT	Biotin-GGG-AASSTKT-CONH2
B41	SEQ ID NO.30	GGGAFAATKT	Biotin-GGG-AFAATKT--CONH2
B42	SEQ ID NO.31	GGGAFASAKA	Biotin-GGG-AFASAKA-CONH2
B43	SEQ ID NO.32	GGGPFSSTAT	Biotin-GGG-PFSSTAT-CONH2
B44	SEQ ID NO.33	GGGAFAAAKA	Biotin-GGG-AFAAAKA-CONH2
B45	SEQ ID NO.34	GGGPFSSAKT	Biotin-GGG-PFSSAKT-CONH2
B46	SEQ ID NO.35	GGGPFSATKT	Biotin-GGG-PFSATKT-CONH2
B47	SEQ ID NO.36	GGGPFSCTKT	Biotin-GGG-PFSCTKT-CONH2
B48	SEQ ID NO.37	GGGPFCSTKT	Biotin-GGG-PFCSTKT-CONH2
B50	SEQ ID NO.38	GAFASTKT	Biotin-G-AFASTKT-CONH2
B51	SEQ ID NO.39	GGGGGAFASTKT	Biotin-GGGGG-AFASTKT-CONH2
B52	SEQ ID NO.40	GGGAFASTKTGRGD	Biotin-GGG-AFASTKT-GRGD-CONH2
B53	SEQ ID NO.41	GGGPFSSTKTGIKVAV	Biotin-GGG-PFSSTKT-GIKVAV-CONH2
B54	SEQ ID NO.42	GGGAFASTKTGIKVAV	Biotin-GGG-AFASTKT-GIKVAV-CONH2
B57	SEQ ID NO.43	GGGAFAK	Biotin-GGG-AFAK-CONH2
B58	SEQ ID NO.44	(GGG)2-KFSSTKT	(Biotin-GGG)2-K-FSSTKT-CONH2
59	SEQ ID NO.45	FGGGAFASTKTGIKVAV	Ac-F-GGG-AFASTKT-GIKVAV-CONH2
60	SEQ ID NO.46	YGGGPFSSTKT	Ac-Y-GGG-PFSSTKT-CONH2
61	SEQ ID NO.47	FGGGAFSSTKTGGGPFSSTKT	Ac-F-GGG-AFSSTKT-CONH2

The self-assembling peptides (SAPs) of the present invention have the amino acid sequences defined in Table 1, in which the one letter IUPAC amino acid code is used (ie. G corresponds to the amino acid Glycine, P corresponds to the amino acid Proline.). Each SAP has a peptide number and a corresponding SEQ ID NO., as above reported in the Table 1.

Each SAP has a corresponding derivated SAP, which is the amino acid sequence with the Biotinilation or Acetilation at the N-terminus and C-terminal amides.

The biotinylated peptides are named with 'B + number'. The other peptides are just numbered.

The SAPs of the present invention are optionally biotinylated and unbiotinylated

sequences at the N-termini and amidated or not at the C-termini, hybrid peptide-peptoid sequences, for a total of 47 tested motifs. The SAPs of the present invention are all linear peptides, with the exception of SEQ ID NO.44 which is a branched peptide with two identical GGG branches.

The subject of the invention is therefore a novel group of low molecular weight self-assembling peptides.

These self-assembling peptides are of synthetic origin and are therefore easy to manufacture in large quantities, and they can be modified chemically and biologically. Such modifications give scientists the chance to construct an ultra-structure promoting cell adhesion and growth.

These peptides have the advantages of being of synthetic origin, and therefore do not have the disadvantages seen in natural peptides such as the tendency to induce inflammatory response and pathogen transfer due to undefined factors that cannot be eliminated by purification prior to implantation, the significant degree of variability between different lots and the difficulty of availability of large scale sources.

The low molecular weight self-assembling peptides of the invention can form hydrogels which are synthetic but naturally inspired and surprisingly form nanostructured materials of easy functionalization and capable of creating microenivorments suited for culturing cells, triggering tissue regeneration and other applications beyond life-sciences such as electrochemical sensing, self-assembling circuits and transistors for computers and construction of three-dimensional nanoscale systems.

Upon exposure to a neutral pH buffer the initial spontaneous, and concentration dependant, self-assembling process is speeded up toward the formation of solid scaffolds, whose stiffness, depending on the peptide sequence, span three orders of magnitude.

Surprisingly the SAPs according to the present invention spontaneously form a number of different and hierarchical aggregated nano- and micro-structures, even though they present such a group of heterogeneous sequences. These peptides assemble into beta-structures (beta-sheets and beta-turns), present aromatic interactions between Phe residues and the tails of the fibers, electrostatic

repulsions (Lys allows to obtain a pH-driven self-assembly), h-bonds formations (Ser,Thr). In most of the peptides pH speed up the self-assembly phenomena spontaneously occurring in water.

The peptides of the present invention surprisingly show a self-healing propensity at the mesoscale, indeed hydrogels re-form solid scaffolds, recovering their initial stiffness, after mechanical rupture.

In fact, in terms of recovery of stiffness of the self-assembled scaffolds, the peptides of the invention self-assemble at multiple hierarchical levels.

The peptides for which self-healing property has been seen are for example B3, 4, B15, B17, B22, B24, B25, B27 and 31 (SEQ ID NO. 1, 2, 7, 8, 10, 11, 12, 13 and 16) giving microscaled tubular structures that could be used for drug delivery by an useful strategy consisting in dissolving peptides in drug loaded solutions prior self-assembly, separating the assembled scaffolds via centrifugation and injecting the self-healing assembled scaffolds *in vivo*.

In a preferred embodiment the self-assembling peptide has an amino acid domain selected from the group consisting of SEQ ID NO. 1, 3, 4, 5, 6, 7, 8, 9, 10, 11, 12, 13, 14, 17, 18, 19, 20 and 21.

In a further preferred embodiment the self-assembling peptide of the invention has the amino acid domain consisting of SEQ ID NO. 14, wherein a propylamine is present between the G in position 3 and the F in position 4. Propylamine, also known as n-propylamine, is an amine with the chemical formula C_3H_9N.

In an even more preferred embodiment the self-assembling peptide has an amino acid domain selected from the group consisting of SEQ ID NO. 1, 3, 4, 5, 6, 7, 8, 9, 10, 11, 12, 13, 14, 17, 18, 19, 20 and 21 wherein the N-terminus is optionally biotinylated.

In an even more preferred embodiment the self-assembling peptide has an amino acid domain selected from the group consisting of SEQ ID NO. 1, 8, 10 and 13 wherein the N-terminus is optionally biotinylated.

In a still more preferred embodiment the self-assembling peptide has the amino acid domain of SEQ ID NO. 11, more preferably wherein the N-terminus is optionally biotinylated.

In a further embodiment the self-assembling peptide of the invention has an amino

acid domain selected from the group consisting of SEQ ID NO. 2, 15 and 16.

In a still further embodiment the self-assembling peptide of the invention has an amino acid domain selected from the group consisting of SEQ ID NO. 2, 15 and 16 wherein the N-terminus is acetylated.

In a still further embodiment the self-assembling peptide of the invention has an amino acid domain selected from the group consisting of SEQ ID NO. 1, 8, 10, 12 and 13.

In a further embodiment the self-assembling peptide of the invention has a number of Glycines of the aminoacid domain of 3 to 8.

In a preferred embodiment the self-assembling peptide of the invention has a number of Glycines of the aminoacid domain of 3 to 6.

By increasing the number of Glycines of the spacers, Biotin acquires more degree of freedom allowing a better exposure and self-orientation for h-bond formation and/or stacking, thus favoring self-assembling. This is why Glycines, ranging in number from 3 to 8, prefereably from 3 to 6, can strongly influence the hierarchical formation of multiple nano- and microstructures.

In a preferred aspect, the present invention concerns the self-assembling peptide (SAP) which consists of an amino acid domain, having from 9 to 14 aminoacids, said domain being:

-GGGPFSSTKT-	SEQ ID N.1
-WGGGPFSSTKT-	SEQ ID N.2
-GGGPFSSTDT-	SEQ ID N.3
-GGGPFSSTNT-	SEQ ID N.4
-GGGPFSSTET-	SEQ ID N.5
-GGGPFSSTQT-	SEQ ID N.6
-GGGAFSSTKT-	SEQ ID N.7
-GGGPFSETKT-	SEQ ID N.8
-GGGAFSSTKTGRGD-	SEQ ID N.9
-GGGPFSSTRT-	SEQ ID N.10
-GGGAFASTKT-	SEQ ID N.11
-GGGGGPFSSTKT-	SEQ ID N.12
-GGGPWSSTKT-	SEQ ID N.13

-GGG(Propylamine)FSSTKT- SEQ ID N.14
-WGGGAFASTKT- SEQ ID N.15
-WGGGAFSSTKT- SEQ ID N.16
-GGGKFSSTPT- SEQ ID N.17
-GGGPKSSTFT- SEQ ID N.18
-GGGPFSSKTT- SEQ ID N.19
-GGGPFSSTTK- SEQ ID N.20
-GGGGPFSSTKT- SEQ ID N.21

In a further preferred aspect, the present invention concerns the self-assembling peptide (SAP) which consists of an amino acid domain, having from 7 to 17 aminoacids, said domain being:

-GGGPFSSTKTGRGD- SEQ ID N.22
-GPFSSTKT- SEQ ID N.23
-GGGAWASTKT- SEQ ID N.24
-GGGAFASTKA- SEQ ID N.25
-FGGGPFSSTKT- SEQ ID N.27
-GGGPYSSTKT- SEQ ID N.28
-GGGAASSTKT- SEQ ID N.29
-GGGAFAATKT- SEQ ID N.30
-GGGAFASAKA- SEQ ID N.31
-GGGPFSSTAT- SEQ ID N.32
-GGGAFAAAKA- SEQ ID N.33
-GGGPFSSAKT- SEQ ID N.34
-GGGPFSATKT- SEQ ID N.35
-GGGPFSCTKT- SEQ ID N.36
-GGGPFCSTKT- SEQ ID N.37
-GAFASTKT- SEQ ID N.38
-GGGGGAFASTKT- SEQ ID N.39
-GGGAFASTKTGRGD- SEQ ID N.40
-GGGPFSSTKTGIKVAV- SEQ ID N.41
-GGGAFASTKTGIKVAV- SEQ ID N.42
-GGGAFAK- SEQ ID N.43

-$(GGG)_2$-KFSSTKT-	SEQ ID N.44
-FGGGAFASTKTGIKVAV-	SEQ ID N.45
-YGGGPFSSTKT-	SEQ ID N.46; or
-FGGGAFSSTKT-	SEQ ID N.47.

In a preferred embodiment the invention regards a hydrogel comprising the self-assembling peptides and a hydrogelating ingredient.

According to a preferred embodiment, the self-assembling peptide polymer comprises at least 2 identical self-assembling peptides of the invention.

A further aspect of the present invention is a self-assembling peptide polymer comprising at least 2 different self-assembling peptides .

A still further embodiment of the invention regards the use of the self-assembling peptide polymer as a medicament.

The invention further regards a tabular nanofiber comprising at least 2 identical self-assembling peptides.

The invention further regards a tabular nanofiber comprising at least 2 different self-assembling peptides.

According to a further embodiment the invention regards a tabular nanofiber, characterised in that it is from 5 to 10μm in length.

According to a still further embodiment the invention regards a complex interwoven membrane made of at least 2 tabular nanofibres.

In a still more preferred embodiment the invention regards 10 μm-long tabular nanofibres which self assemble into complex interwoven membranes of from 0.5 to 4 μm in width.

The peptides of the present invention surprisingly self-aggregate and arrange at the nanoscale in structures ranging from tabular fibers to twisted coils and hierarchically assembled sheets, showing a high mechanical stiffness of the assembled scaffolds.

A further embodiment of the invention regards therefore a self-assembled nanostructure consisting of 2 or more identical peptides.

A further embodiment of the invention regards a self-assembled nanostructure consisting of 2 or more different peptides.

A further embodiment of the invention regards the self-assembled nanostructure

having a hollow cavity and the use of such a self-assembled nanostructure for the release of small molecular drugs.

Such small molecular drugs can be confined in scaffold hollow cavities and eventually interact weakly with the net surface charges of the self-assembled nanostructures thus being released slowly.

Additionally, being some biotins available for binding with streptavidin (tagging tests were successfully conducted in vivo to track bioabsorption time in animals), biotinylated peptides can be functionalized, by using streptavidin or avidin as linkers, with additional biotinylated functional motifs or biotinylated drugs or cytokines to obtain a slow delivery in vivo.

In a still more preferred embodiment the invention regards a pharmaceutical composition comprising at least one polymer according to the invention and a pharmaceutically bioactive excipient.

Exemplary pharmaceutically acceptable excipients include any and all solvents, dispersion media, diluents, or other liquid vehicles, dispersion or suspension aids, surface active agents, isotonic agents, thickening or emulsifying agents, preservatives, solid binders, lubricants and the like, as suited to the particular form of administration and dosage.

Further the invention regards the use of the hydrogel for use as a scaffold for in vitro cell culture.

Further the invention regards the use of the hydrogel for in vitro cell culture in 2 and 3 dimensions. These hydrogels are very similar to the fibrous component of the extra cellular matrix, which makes them capable of supporting cell cultures in two dimensions (2-D) and three dimensions (3-D).

A further aspect of the invention is the use of the hydrogel according to the invention as a scaffold for the in vitro growth and differentiation of human neural stem cells (hNSCs) to assess their potential for *in vitro* cell cultures and *in vivo* nervous tissue regeneration.

A still further aspect of the invention is the use of the hydrogel according to the invention as a scaffold for the in vitro growth and differentiation of murine neural stem cells (hNSCs) to assess their potential for *in vitro* cell cultures and *in vivo* nervous tissue regeneration.

In a still further aspect the invention regards the use of the hydrogel according to the invention for in vivo nervous regeneration.

In a still further aspect the invention regards the use of the hydrogel according to the invention for hemostasis.

In a still further aspect the invention regards the use of the hydrogel according to claim 4 in regenerative medicine applications and for delivering drugs in vivo, for tissue engineering and for triggering tissue regeneration.

A self-assembling peptide of the invention, may be used to treat a variety of tissue defects and diseases. Hydrogels, either with or without cells growing on the surface or encapsulated within may be implanted into the body, e.g., surgically or using any other type of suitable procedure. Other routes, including oral, percutaneous, intramuscular, intravenous, and subcutaneous may be employed. One of ordinary skill in the art will be able to select an appropriate delivery technique.

In general, SAPs of the invention may be useful in any situation involving injury or damage to tissue. Such injury may occur as a result of surgery, trauma, tumor, degenerative disease, or other diseases or conditions. The injury may, but need not, involve death of cells. The SAPs are useful to restore structural and/or functional integrity to the tissue, i.e., to aid in restoring the tissue to the functional or structural condition that existed prior to the injury. Certain injuries may result in physical barriers that can impede regeneration or repair of tissue. Such barriers may include areas of necrosis, cavitation, or scar tissue formation. In certain embodiments of the invention introducing the materials described herein at a site of injury allows cell or tissue growth from a location proximal to the site of injury or barrier to a location distal to the site of injury or barrier.

Certain SAPs of the present invention may be used to ameliorate the effects of disease or degeneration of an organ, to repair an injury to an organ or other body structure or to form an organ or other body structure. Such organs or body structures include, but are not necessarily limited to, vascular tissue, brain, nervous tissue, peripheral nerves, cartilage, esophagus, fallopian tube, heart, intestines, gallbladder, kidney, liver, lung, ovaries, pancreas, prostate, bladder, bone, spinal cord, spleen, stomach, testes, thymus, thyroid, trachea, ureter,

urethra, uterus, and skin.

The present SAPs may also be used in dermatology as fillers for use in aesthetical and cosmetic techniques, to counteract wrinkles and the most common signs of ageing.

SAPs according to the present invention can be used in particular in the form of hydrogels, as filling materials in order to restore the skins youthful aspect, and reduce fine lines and wrinkles.

In general, a variety of devices may be used to introduce the hydrogels of the invention at the site of injury. Delivery via a syringe is one convenient technique. SAPs can also be introduced by catheter or directly at a site of surgery. In other embodiments of the invention hydrogel formation is allowed to occur in vitro and the hydrogel is introduced into the body.

The self-assembling peptides of the invention may be used to promote formation of a layer of vascular endothelium at a site of injury, e.g., following a procedure such as angioplasty. They can also be used as coating materials, e.g., for devices such as vascular grafts or stents, to promote endothelialization. In an alternate approach, the SAPs form a layer on the inner surface of an artificial conduit such as an artificial blood vessel. Endothelial cells are cultured on the layer formed by the self-assembled peptides for a period of time. The cells secrete ECM components. The cells may then be removed, leaving behind an intact basement membrane layer containing ECM molecules synthesized by the cells.

A still further aspect of the invention is the use of such peptides as molecular switches or devices sensitive to pH, concentration and temperature.

The self-assembling phenomena of the novel peptides obtained are illustrated and demonstrated in the Examples 1 - 6 described in the present invention.

EXAMPLE 1

Synthesis and purification of peptides of the present invention

Each peptides of the present invention was synthesized on a 0.05 mmol scale with standard fluorenyl methoxy carbonyl solid-phase techniques using an AAPTEC peptide synthesizer. Rink amide resin (0.6 mmol/g substitution) was used to produce C-terminal amides; amino acids were dissolved in 0.4 M NMP with 0.4 M HoBt; 0.5 M Biotin with 0.4 M HoBt in DMSO solution was used for biotinylation

step.

The peptides were then cleaved from the resin and deprotected with 4ml of 95% trifluoroacetic acid (TFA), 2,5% water and 2,5% triisopropylsilane. The cleaved peptides were precipitated, washed several times with cold diethyl ether and dissolved in 20-25% of acetonitrile solution prior to be lyophilized and stored at -20 °C. Crude peptides were analyzed and purified by reverse phase HPLC using a Varian Galaxie system equipped with an analytical and semi-preparative C18 columns. Eluents were 0,1% (v/v) TFA in water (Buffer A) and 0,1% (v/v) TFA in acetonitrile (Buffer B). Starting conditions were 0% buffer A and 100% buffer B and the gradient developed with a linear increase in buffer B. In 40 minutes gradient went to 45% buffer B. Molecular weight of the peptides was confirmed with MALDI-TOF mass spectrometry (4800 Applied Biosystems).

Schematic representation of the main sequence variations in figure 1.

The acetylated BMHP sequence (Ac-PFSSTKT-CONH2) and a Gly added version (Ac-GGGPFSSTKT-CONH2) were synthesized and purified to assess their propensity in forming membranes or scaffolds when dissolved in distilled water and in phosphate-buffered saline solution (PBS) pH 7.4 at the macroscale.

Biotin, a water-soluble vitamin, acts as a cofactor in a number of important biochemical metabolic reactions and pathways related to cell signalling, gene expression, and chromatin structure (10). Multiple conformational ensembles of biotin, ranging from extended to folded states, have been found in solution (11). The latter structures are stabilized by hydrogen bonding between the ureido group and the valeryl carboxylic acid side chain. SEQ ID NO.1 was tagged with biotin (peptide B3: Biot-GGGPFSSTKT-CONH2), obtaining a viscous and opaque solution (at 3% w/v concentration) shifting to solid scaffold when exposed to neutral pH buffer. Consequently, in order to asses the importance of each residue/feature of the discovered SAP 48 additional new peptides representing specific variations of peptide B3 (figure 1) were synthesized.

In detail, biotin was replaced with tryptophan (peptides 4, 30, 31), with phenylalanine (peptides 37, 59, 61) or with tyrosine (peptide 60). Other modifications comprise proline substitution with alanine (peptides B15, B19, B24, 30 and 31, B32, B33, B40, B41, B42, B44, B50, B51, B52, B54, B55, B57) or with

propylamine (peptide B28) to give more linearity to the molecule backbone. B28 (SEQ ID NO. 14) has a peptoid residue, a propylamine, which is inserted between the G in position 3 and the F in position 4 instead of a proline aminoacid: this guarantees the same number of carbon atoms of side chain without the characteristic α-carbon of proline. The choice of testing propylamine was made in optic of designing new hybrid sequences, made of peptides and peptoids (12), class of oligomers recently driving widespread interest, amenable of easy functionalization with bioactive motifs at their side-chains. Another option for the functionalization of these SAPs was to add a cell adhesion motif like RGD (13) or IKVAV at the C-termini (peptides B18, B19, B52, B53, B54, 59) via a Gly-spacer.

The importance of H-bond forming serines in self-assembling was assessed via their substitution with alanines (peptides B24, 30, B32, B33, B41, B42, B44, B46, B54, B55, B52, B50, B51, B57). Serines were also substituted with cystein in B47 and B48.

Peptides total net charge at neutral pH was changed by substituting a serine 8 with glutamic Acid (B17) or by replacing lysine with opposite charged residues (B10 and B12) or, alternatively, neutral residues (B11, B13 and B43). Lysine was also replaced with positively charged arginine (B22). Phenylalanine was substituted with tryptophane (B27, B32), with tyrosine (B39) or with alanine (B40).

The G-spacer length was varied (between the N-termini and the BMHP fragment) from 0 (Biot–PFSSTKT-CONH2) to 1 (B29, B50) , to 3 (peptide B3) and 5 residues (peptides B25 and B51). While in case of the first sequence no self-assembling was detected at both nano- and mesoscales, that was not the case for peptides B3, B25, B29, B50 and B51. A branched peptide (B58) was introduced to act as knot between assembled nanostructure thus altering the biomechanical properties of the other hydrogels when dissolved with any of the other linear peptides. Lysine was shifted in different position within the sequence (B64, B65, B66, B67)

Some of the proposed modifications were combined together to assess their synergistic effect, if any.

EXAMPLE 2

Rheological tests

Rheological properties were determined for the peptides of the invention, using a

controlled stress TA Instruments AR-2000ex rheometer (TAInstruments). A cone-and-plate geometry (acrylic cone diameter, 20 mm; angle, 1°; truncation gap 34 μm) was used. All measurements were obtained at a constant monitored temperature of 25°C. Preliminary strain sweeps were performed for each sample to define the linear viscoelastic region, thus ensuring that moduli were independent of strain. Time sweeps, after addition of PBS (1x) were recorded at constant angular frequency (ω=1 Hz). Frequency sweeps, both for peptide water solutions and for self-assembled scaffolds, were performed with the instrument in oscillatory mode at controlled strain of 1%. Final: onset point of rupture was calculated by linear interpolation and subsequent determination of the intersection of the G' modes in the linear region and at material rupture respectively. G' values were averaged in the 1-100 Hz region and between n=3 independent replicates. During self-healing tests the self-assembled scaffold was torn by applying a strain sweep (0.01% - 1000% strain range) at 1 Hz oscillatory frequency. G' values were recorded in frequency sweep mode (at 1 % strain) or, in time sweep mode (at 1 Hz and at 1% strain), before and after the strain sweep step, subsequent observations were performed every half hour or, in case of time sweep test, every 30 seconds.

Values for all peptides, averaged in the 1-100 Hz range, are reported in Figure 2d. In all of the SAPs the difference between the storage moduli measured before and after PBS addition spanned from two to four orders of magnitude, proving the dramatic biomechanical changes taking place during scaffold gelation. Peptide B3 (1%) yielded a solid stiff scaffold (G'=2917 Pa), supporting the idea that ionic charges may screen the electrostatic repulsions given by positively charged lysine residues and speed up the spontaneous ongoing self-assembling process, on its turn giving an already viscous (G'=67 Pa) and opaque solution at day 1. Among the peptides giving soft scaffold (100 Pa -1000 Pa range) peptides 4, B19, B25, B28 and 30 were included. On the opposite side, SAPs yielding solid stiff scaffolds are B15, B22, B24, B27 and 31 (5000 Pa - 9000 Pa range).

Additionally, in case of B15, Proline substitution did produce a stiff solid scaffold (G'=8500 Pa) while for B24, the simultaneous substitution of proline and serine 7, the latter important in self-assembling for its role in H-bonds formation, with a couple of alanines, brought the overall scaffold stiffness to values higher (G'=6502

Pa) than peptide B3. On the other side, proline substitution with a peptoid residue (B28) decreased the assembled scaffold stiffness and increased the minimum necessary peptide concentration for gelation (namely 3% w/v).

G-spacer variations affected the final scaffold stiffness (B25), while its absence prevented the tested peptide from forming any scaffolds.

Biotin substitution with tryptophan (peptides 4 and 30) dramatically decreased G' (if compared to B3 and B24 respectively) and the rate of the viscosity increments of the peptide solution before pH shift. Biotin deletion prevented any scaffold formation instead (peptide 2).

Macro-scale characterization of the peptides of the invention and rheology

All of the synthesized peptides are soluble at 1% w/v concentration in distilled water and in acid (0.1 M HCl) solutions. Peptides B10, B11, B12 and B13, are immediately self-assembling with dissolution in water.

The tested peptides solutions appearance ranged from peptides giving clear liquid solutions (e.g. 4, B15, B19, B25, B28, 30) to samples which become opaque in 1 to 7 days after dissolution (e.g.B3, B17, B22, B24, B27, 31) as shown in figure 2a (I). Most of the liquid solutions increased in viscosity over the first week after dissolution, however after ten days in water no appreciable changes happened at the macroscale. Upon exposure to PBS (1x) the following peptides yielded solid scaffolds similarly to figure 2a (II): B3, 4, B15, B17, B19, B22, B24, B25, B27, B28, 30, 31, B32, B33, B34, 37, B39, B40, B41, B42, B43, B44, B45, B46, B47, B48, B50, B51, B52, B53, B54, B57, B58, 59, 60, 61, B64 and B65 (black font in figure 1).

The mechanical properties of the synthesized peptides were tested with a cone-and-plate rheometer. Firstly, the G' dependence of peptide water solutions on concentration increments, and consequently aggregation kinetics, was assessed as shown in figure 2b. Clearly peptide B3 shows different mean G' values (averaged in the 1-60 Hz frequency range) starting from the day of dissolution (day 0) and reaching a plateau at day 2 for 3% concentration and still increasing at day 5 when dissolved at 2% concentration. This shows that rate of storage moduli increments increases along with peptide concentration.

Nonetheless, keeping constant the observation time, the storage moduli of peptide

solutions previously dissolved (the day before) at 3% w/v were measured. Measurements were obtained of these peptide solutions, further diluted to 1% w/v at the same day of the experiment (unless otherwise specified), and, after addition of PBS, of the formed scaffolds. When the proposed standard conditions were not optimal for some of such heterogeneous ensemble of SAPs possessing different kinetics of self-assembling, (e.g. too viscous solutions for reliable user handling or poor scaffold gelation), it was chosen to increase the peptide concentration (B19, B28, 30 and 31) or to wait for more time for the spontaneous self-assembling to take place (4, B27 and 30) before triggering scaffold formation by varying the pH, or, conversely, to lower down the concentration (B3, B22 and B24) because of the hardly reproducible handling by the user of too highly viscous solutions.

For B10, B11, B12 and B13, yielding solutions of interspersed fragments of self-assembled scaffolds, measurements were unreliable and not reported.

Control peptide B7, having the amino acid sequence: Biot-PFSSTKT-CONH2, did not give a solid scaffold at the macro-scale observations and did not show any steady G' increase after addition of neutral pH buffer in figure 2c) and was characterized by very low and not linear G' and G'' values. As to the other peptides a stable linear frequency response (in the 1-100 Hz range) was detected, with G' values (representing the elastic character of the materials) well above G'' values (representing the viscous character of the materials):hence resembling the typical responses of solid structures (see figure 2c).

EXAMPLE 3

Atomic Force Microscopy

Each peptide of the present invention was analysed by Atomic Force Microscopy. Peptides were dissolved in distilled water (GIBCO), at a concentration of 3% w/v one day prior imaging. Imaging and measurements were collected at day 1, day 3, day 7 and so on (maximum observation time was 30 days after dissolution). The same day of imaging peptide solutions were diluted (in a ratio of 1 to 3 or more if fiber density was too high), 2 μl of these solutions were placed on mica muscovite substrates and kept at room temperature for 2 minutes. The mica surfaces were then rinsed with distilled water to remove loosely bound peptides and solution was let to evaporate for 30 minutes. AFM images were collected in tapping™ mode by

a MultiMode Nanoscope IIIa (Digital Instruments) using single-beam silicon cantilever probes (Veeco RTESP: resonance frequency 300 KHz, nominal tip radius of curvature 10nm, forces constant 40 N/m). If necessary, images (1024x1024 resolution) were subjected to flattening. When tabular nanofibers were detected and fiber height was between 1 and 1.5 nm, i.e. far lower than the tip radius (10 nm), tip convolution effect was corrected with the formula:

$$\Delta x = \sqrt{2[h(2r_t - h)]} \quad (1)$$

Where Δx is the width broadening effect, h is the nanofiber height, and rt is for tip radius.

Results are presented as means averaged over more than 100 measurements.

Atomic Force Microscope (AFM) imaging and characterization of the peptides of the invention.

Deep characterization of the spontaneous self-assembly at the nano- and micro-scale required imaging with AFM of all of the synthesized peptides. The self-assembling peptides gave rise to various structures that could be grouped in six categories as represented in figure 3.

Self-assembling peptides B64, B65, B66 and B67 formed twisted nanofiber formations (60 nm pitch, left-handed) since 1 day post dissolution, and also self-assembled giving a hydrogel upon exposure to PBS (figure 3a).

Proline-free peptides B15, B24, B32, B33, B40, B41, B42, B54, B58, 59, B44 and 61 gave rise to tabular long fibers (ranging from 5 μm to 10 μm in length). Nanofiber heights were of 1.6 nm and multiples, while widths were of 8-9 nm and multiples, given by fibers clamped together laterally (figure 3b). Average fiber dimensions did not change significantly at the tested time-points (up to 10 days after dissolution).

In case of peptide 4, 37 and 60 thicker fibers (minimum width of 30 nm), likely made of coiled thinner intermediate filaments similar to those imaged with B15 and B24, were imaged. Moreover, mostly twisted fibers were present (see figure 3c), showing a left-handed pitch ranging from 100 to 150 nm (measured as top-to-top horizontal distances). Heights were of 2.5 nm and multiples (measured at the slope bottoms), with a vertical span of 5 nm (registered as a top-to-bottom vertical

distance) in the profile shape of the same twisted fiber. Notably, at the selected observation time points of day 1, 3 and 10 the density of imaged fibers (i.e. number of fibers per imaged field) increased over time, consistently with the previously observed slow kinetic of viscosity increments of peptide 4.

Similar fibers but with different features were seen for peptides B18, B19, B25, B28, B29, 30, 31, B45, B50, B51, B52 and B53 (figure 2e). In this set of peptides the twisted fiber width was 15 nm and 30 nm while heights could be grouped in 6 nm (bottom) – 11 nm (top) and 12 nm (bottom)-19 nm (top), giving an approximate vertical span of 6 nm between top and bottom fibers (only 2 nm in the case of 30). Pitches of the left-handed twisted fibers measured between 80 nm and 110 nm, except for B28 (whose fiber pitches ranged from 30 nm to 40 nm). In the case of peptide B25 side-by-side packed fibers were occasionally seen, however this fact might be just a side effect of the sample prepared through water evaporation. In the first days after dissolution B19 also formed flat intermediate-fibers that eventually wrapped in the days after. For peptide 31 intermediate-fibers (height: 3.6 nm to 4.3 nm; pitch: 35 nm) gradually packed together giving similar eventual nanofibers.

Necessarily, peptides B10, B11, B12, B13 and B43 were grouped together because of the poor handling which, at least, allowed for imaging of some scattered chunks of aggregated left-handed twisted fibers, as can be seen in figure 3d. In this case the immediate self-assembling, given by the neutral or negative total net charge, immediately caused filaments to bundle together, lowering down their potential for making solid scaffolds.

In the last group intermediate left-handed twisted protofibrils (figure 3f (I); width 8.5 nm and multiples; height 2-2.8 nm; 28-30 nm pitch for B3 and B22, 90-110 nm for B17 and B27) of peptides B3, B17, B2, B27, B34, B39, B46, B47, B48 and B57 aligned side-by-side and hierarchically self-organized in bigger ribbon-like long structures (featuring highly variable pitches and more than 12 μm long structures) (figure 3f (II)) characterized by both left and right turns, that, on their turn, helically coil to form straight tubular structures (figure 3f (III)) and eventually double- or multi-layered flat sheets (figure 3f (IV)), giving structures as high as 3-3.6 nm (3f(III)) and 6.4 or 14 nm (3f (IV)) respectively. Particularly in the last group the

kinetic of the hierarchically self-assembling was clearly detectable up to 10 days following dissolution (smaller protofibrils were followed by bigger ribbons, tubular structures and flat sheets): after that time growing micro-structures, as big as several squared microns, are affected by sample preparation thus not discussed here.

The members of this last group of SAPs all share the presence of biotin, the triplet of glycines, proline 5 except for the B57 peptide, an aromatic residue at position 6, serine 7 or serine 8 (except for B57) and a positively charged residue at position 10 (or 8 for B57). Thus, in general, the following generic sequence, bio-GGG-$PX_1SXxXxX_3Xx$, (where X_1=aromatic residue; Xx=h-bond forming residues; X_3=positively charged residue) can actually self-assemble at multiple levels of arrangements hierarchically. Other substitutions with similar residues will be required to highlight more generic specification to this type of self-assembling to take place.

The dipeptide Phe-Phe forms tubular structures, which directly indicated the importance of the aromatic interaction for structure formation (14), and the self-assembled ultrastructure dependence of tetrapeptides on the relative positions of proline and phenylalanine residues, suggesting a crucial role of pyrrolidine-aromatic and π–π interactions in fiber formation.

EXAMPLE 4

X-Ray Diffraction analysis (XRD)

Each peptide of the present invention was analysed with X-ray diffraction.

X-ray diffraction data were collected at a multiple-wavelength anomalous diffraction and monochromatic macromolecular crystallography beamline 8.3.1, at the Advanced Light Source located at Lawrence Berkeley National Laboratory. Beamline 8.3.1 has a 5 tesla single pole superbend source with an energy range of 2.4-18 keV. Data were collected with a 3 x 3 CCD array (ADSC Q315r) detector at a wavelength of 1.1159 Å. Data sets were collected at 200-mm distances with 40s exposure times and 1 degree oscillations on a bulk sample of SAPs dissolved the day before at 3% w/v concentration. In case of partially soluble peptides higher concentrations were adopted and the insoluble samples were discarded. Peptide fiber containing solutions were centrifuged at 12,000 rpm for 10 minutes. The

resulting concentrated solution was then dropped on a 0.2-0.3 mm diameter nylon loop. Data were processed in Igor Pro 6.0 with a silver behenate (AgBE) standard.

Circular Dichroism (CD) analysis

Far-UV CD spectra of each of the peptides of the present invention are recorded between 190nm – 260nm at room temperature on an Aviv 62DS spectrometer. All measurements were carried out in 1-mm quartz cuvette in distilled water. Spectra are from accumulation of 3 scans. Blank spectra of the buffer without sample are subtracted. CD spectra of peptide samples at 0.02%, 0.04% and 0.06% w/v concentrations are collected at one day after dissolution in water. Spectra are recorded in 2-nm steps, averaged over 4 seconds and normalized into Delta Epsilon units. Protein structures were deconvoluted by using the CD Spectra Deconvolution Software 2.1 using 33 base spectra of known proteins.

X-Ray Diffraction (XRD) data and CD characterization of the peptides of the invention

The following peptides were tested for XRD studies: B3, 4, B12, B13, B15, and B19, B25, B33, B34, B47, B48, B53. Measurements were taken of samples dissolved the day before the experiments at 3% concentration. Most of the tested peptides gave isotropic rings with the maximum intensity at approximately 4.7 Å distance, usually ascribed to the h-bonding spacing between β-strands, typical of unaligned β-sheet forming fibers (see figure 4a). Another clearly visible ring was found at 3-1.7 nm distance interval. Additionally, radial integration of the patterns revealed other diffraction peaks (figure 4b), shared by all peptides, at 3.7-3.8 Å, typical van der Waals distance of packed peptide side-chains, and 2.3-2.4 Å, considered as the second order of the 4.7 Å peak. Nonetheless these maxima gave a much less intense signal if compared to the 4.7 Å peak.

Notably, B3, B12, B13, B34, B47, B53 peptides showed a medium intensity peak at 2.1 nm (arrow in figure 5a), while peptides B19 and 4 gave a peak at 2.86 nm and 2.35 nm respectively. In B15, B33, B48 the maxima was detected at 1.73 nm. In B25 we had a peak at 1.96 nm. Beside B19, for whom likely protofibrils were simply not detected, and B12 and B13, where reliable AFM measurements could not be obtained, the peaks at distance greater than 1.5 nm were consistent with

nanofiber heights measured via AFM. Different heights resembled different molecular arrangements giving twisted or tabular fibers, or, at the higher level of self-organization, ribbon-like tubular structures. Lastly peaks at 5.2 Å, like in B3, or, in general, between 5 Å and 8 Å, for peptides B12, B13, B15, B19, B25, B33, B34, B47, B48 and B53 may be interpreted as inter-molecular aromatic interactions: interactions not seen in the case of biotin substitution with tryptophane in peptide 4.

Circular Dichroism (CD) spectroscopy studies were run to asses the secondary structures, spontaneously formed by the following self-assembling peptides: B3, 4, B15, B17, B19, B22, B24, B25 B27, B28, 31, 30, B33. All of the tested peptides dissolved in pure water showed spectra (similar to that one depicted in figure 4b for peptide B24), that, once deconvolved, gave more than 50% presence of β-structures, thus supporting the previous interpretation of the 4.7 Å distance.

EXAMPLE 5

In vitro tests: neural stem cells seeding and imaging

Neural precursor cultures are established and expanded as previously described (15, 16). Human neural stem cells (NSCs) were isolated from the central nervous system, in particular from the diencephalon and the cerebral cortex of human brain 10.5 weeks from conception. The modalities for obtaining the primary tissue are in agreement with the guidelines of the European Network for Transplantation (NECTAR).

In vitro tests were performed following a previously adopted methodology (5). Briefly, cells (at a concentration of $6x10^4$ cells/cm^2) were seeded on the top-surface of each assembled scaffold previously assembled into 96 multiwells. Initially, cells were cultured with basal medium supplemented with βFGF (10 ng/ml), added to enhance neuronal progeny differentiation. At 3 days in vitro (DIV), βFGF medium was replaced with Leukemia Inhibitory Factor (LIF, Chemicon) (20 ng/ml) and Brain Derived Neurotrophic Factor (BDNF, Peprotech) (20 ng/ml). Fresh medium was added every three days. Positive and negative controls consisted of Cultrex-BME® substrate (R&D systems) (1:100 dilution in basal medium) and untreated bottom well surfaces respectively.

Live/Dead cell imaging (MolecularProbes) was obtained by incubating cells

cultured for 10 days with a staining solution containing 2.0 μM calcein AM and 4.0 μM ethidium homodimer in PBS at 37 °C for 60 min and visualized by inverted fluorescence microscope (Zeiss).

Cell viability was quantified via CellTiter 96® Aqueous Proliferation Assay (Promega, Madison, WI) at 7 DIV as recommended in the Promega protocol. After calibrating the linear response between the cell number and absorbance values, proliferated cell populations were quantified (n=6) by using a Vmax microplate reader (Molecular Devices, Sunnyvale, CA) at 490 nm wavelength. Values, reported as means ± standard error of the mean, were blanked to their respective controls consisting of same substrates and cell culture media without cells.

To assess the differentiated phenotypes cells were stained at 14 DIV for βIIITubulin (Covance, 1:750), GFAP (Chemicon, 1:3000), MAP2 (Sigma, 1:200), GalC (Chemicon, 1:200) and O_4 (Chemicon, 1:200), subsequently marked with Cy3 (Jackson, 1:1000) and Alexa 488 (Molecular Probes, 1:1000) secondary antibodies. In details, cells were fixed in paraformaldehyde 4% for 15 minutes, permeabilized 10 minutes with PBS/0,1% Triton X-100 and blocked for 1 hour with PBS/20% Normal Goat Serum. Samples were incubated overnight in PBS/10% Normal Goat Serum solutions of primary antibodies and incubated overnight at +4° C. After several washes with PBS, secondary antibodies diluted in PBS/10% Normal Goat Serum were applied for 1 hour. Cell nuclei were counterstained with DAPI, samples were mounted with FluorSave reagent (Calbiochem) and samples were visualized and analyzed with a fluorescence microscope. $\beta III Tubulin^+$, $GFAP^+$, $GalC^+/O_4^+$ and $MAP2^+$ cells were quantified by counting positive cells in 4 independent experiments

Scaffolds for in vitro cell cultures

To assess the potential of the proposed SAPs for cell cultures and, more generally, for regenerative medicine, a two-dimensional cell culture protocol already developed for RADA16-I-like peptides was adapted (5). Briefly, human Neural Stem Cells (hNSCs), mechanically dissociated 1 day before plating, were seeded and cultured for one week in vitro over self-assembled scaffolds of B3, 4, B15, B17, B19, B22, B24, B25, B27, B28, 30, 31 and over non-coated tissue culture plastic wells (negative control). Phase contrast imaging revealed an

heterogeneous degree of spreading of cultured hNSCs over the various peptides (see figure 5a), ranging from proliferated cell clusters (in case of B17, B22 and B28), to branched cells (B3, B15 and 31) to adhered and differentiating hNSCs (B24).

Imaging of calcein-AM-labeled living cells and ethidium-homodimer-labeled dead cells cultured for 10 days showed highly viable cells clustered in round-shaped clusters in case of plastic (figure 5b), clamped in poorly branched aggregates (B22) or distributed throughout the gel top surface (B24). The negligible percentage of dead cells (red dots) seems to refute a possible cytotoxic effect of these materials.

CellTiter assay results, resumed in figure 5c, showed that most of the substrates improved hNSC viability when compared to negative control. In particular, B24 showed the highest values of viable NSCs at 7 DIV, while in differentiation experiments at 14 DIV, the percentages of βIIITubulin$^+$, MAP2$^+$, GalC/O4$^+$ and GFAP$^+$ cells (Figure 5d) were comparable to standard hNSC differentiation data obtained with animal extracts (5).

In most of the self-assembled scaffolds the original BMHP sequence, already proved to stimulate hNSC proliferation and differentiation (5), is here likely not fully exposed or modified in the crucial residues (B17, B22, B25, B27, 30) for cell membrane receptor binding: in particular in B3, B17, B22 and B27 hierarchical aggregation may 'bury' the PFSSTKT-like motif within complex structures impairing the correct exposure of whole active sequence. This is not the case of B24 and B15, where the tabular structure of β-sheet nanofibers probably allows a better solvent exposure of the functional motifs.

Biotin-free peptides 4 and 31 produced results comparable to the biotinilated peptides.

The addition of the RGD motif adopted in B19 can be considered as the proof-of-concept, giving results significantly different from negative control ($P<0.002$: paired t-test), that, with the specific set of selected residues, these SAPs may be effectively functionalized without preventing peptide self-assembling.

B28 achieved a cell population comparable to those of the other peptides regardless of its partially unnatural sequence.

B24 supported hNSCs differentiation toward neurons (βIIITubulin and MAP2 markers), astrocytes (GFAP marker) and oligodendrocytes (GalC/O_4 markers), the three main cell phenotypes of the central nervous system.

Taken together these results demonstrate that these SAPs can foster hNSC survival, spreading and differentiation: quality that increases their potential as tool for 2D and 3D cell cultures and regenerative medicine.

Example 6.

Self-healing materials

Interestingly, most of the self-assembling peptides were also verified for their self-healing propensity, namely, the capability of switching back to fully formed hydrogels with viscoelastic properties similar to that of the pre-strained assembled gel. Solid scaffolds were obtained via addition of PBS (1x) in a cone-and-plate rheometer; we measured the storage modulus, the samples were subjected to a strain sweep (0.01% to 1000%) until and far beyond rupture occurred (i.e. monitoring the sudden drop of G' value). Samples were then left in place (keeping them hydrated with PBS) and their G' were measured every 30 minutes via frequency sweep tests in the range of 0.1 Hz to 60 Hz. As a negative control KLD-12, a well-known SAP, was tested (4, 6). For peptides B17 (1% w/v/ concentration) a gradual increase was detected, till full recovery, of the initial G' values at 120' after rupture as can be seen in figure 6a, while, in case of KLD-12, storage moduli values were similar to those registered immediately after breakage (figure 6c). In figure 6b peptide B25 (3% w/v concentration) was assessed for self-healing in a time sweep mode, every 30 seconds, at 1 Hz and at 1% strain. Values of G' recovered after 100 minutes (1000 Pa) and steadily plateaued over time. For peptides B3, B22, B25 and B27 full recovery was obtained at different time intervals after rupture, ranging from 60' to 240'. Similar results were confirmed by multiple independent experiments, but at different time ranges, for all of the self-assembling peptides except for B19 and B28.

Additionally, multiple and consecutive mechanical breakages were obtained by stirring the scaffolds, previously self-assembled in transparent cuvettes (as seen in figure 2a), via pipette tips and subsequent vortexing. Samples were checked for rupture by tilting. After a maximum of four hours all of the samples returned to their

solidified gel appearance. This healing could be repeated at will.

It must be stated that the self-healing phenomenon is probably a re-arrangement, at the meso-scale, of the high-level aggregated structures (sheets and ribbon-like structures): the smaller proto-fibrillary structures seen at the high magnification imaging at AFM are preserved in these tests. Scaffolds coming from the above mentioned peptides are likely formed by transient physical cross-links that form between assembled nanostructures at the higher level of the hierarchically self-aggregation, i.e. among straight tubular fibers and sheets.

Example 7

Scaffolds for tissue engineering applications

To test if the SAPs according to the present invention show any toxicity when used *in vivo* we assessed the tissue reaction to multiple injections of B24 into the spinal cord of rats. All procedures involving animals were performed according to EC guidelines (EC Council Directive 86/609, 1987), to the Italian legislation on animal experimentation (Decreto L. vo 116/92) and to protocols approved by the Animal Care and Use Committee of the University of Milan-Bicocca (IACUC 37/07).

Female Sprague-Dawley rats weighting 200-250 gr (Charles River Laboratories) were divided into two groups: 1) animals receiving injections of saline solution (control group, n=3) and 2) animals treated with B24 (n=3). In the case of long term observations (1 month) similar injections of B24 were used (n=2). Rats were anesthetized with an intraperitoneal injection of ketamine (80 mg/kg) and xylazine (10 mg/kg). The spinal cord was exposed at the T9-T10 level, and, after laminectomy, animals were injected with B24 (1% aqueous solution) or saline solution using a Hamilton syringe held *via* a micromanipulator. The solutions were delivered at distances of 500 µm, and two injections of 0,5 µl each were made at each interval, for a total dose of 3 µl. After injection, the muscles were sutured and the skin was closed with wound clips. Rats were treated daily with analgesic (carprofen, 5 mg/kg) and antibiotic (enrofloxacin, 5 mg/kg). 3 days after surgery (for toxicity tests) or 1 month after surgery (nervous regeneration tests) animals were sacrificed by transcardial perfusion with 4% paraformaldehyde. Spinal cords were removed, embedded in OCT, frozen and sliced into 16 µm thick longitudinal sections. For immunofluorescence analysis slices were permeabilized and blocked

with PBS/0,3% TritonX-100/10% Normal Goat Serum (NGS) for 1 hour at room temperature. Then slices were incubated 16 hours with the following primary antibodies diluted in PBS/0,3% TritonX-100/1% NGS: anti-CD68 (1:500, Serotec), anti-βIIITubulin (1:400, Covance), anti-growth associated protein 43 (GAP-43) (1:200, Millipore) and anti-SMI 32 (1:1000, Covance). Goat anti Mouse Alexa 488 (Molecular Probes; 1:1000) and anti-rabbit Cy3 (Jackson, 1:1000) secondary antibodies diluted in PBS/0,3% TritonX-100/1% NGS were used for signal detection by incubating slices for 1 hour. Cell nuclei were counterstained with DAPI (Roche) and slices were mounted with Fluorsave (Calbiochem). For short-term histochemical analysis, slices were stained with hematoxylin/eosin. Tunel assay was performed using the *In Situ* Cell Death Detection Kit (Roche) according to the manufacturer's instructions. Images were taken with Zeiss Apotome Observer Z.1.

For each staining analyses were performed on six contiguous slices of the injection sites per each animal.

Strikingly B24 prevented the hematoma physiologically forming after micro-injections found in control group (Figure 7F,G and 7A,B respectively). Three days after injection, the spinal cord tissue of B24-injected animals displayed a negligible number of infiltrated macrophages and apoptotic cells in and around the area of the injections (Figure 7H,I respectively) if compared to saline-injected animals (Figure 7C,D respectively). The neurofilament H dephosphorilated nervous fibers were equally present in saline-injected and in B24-treated animals (Figure 7E,J). Summarizing, B24 prevented hematoma formation due to experimental surgery, it did not enhance either significant macrophages infiltration or apoptotic cell death and did not exacerbate nervous fibers degeneration when compared to saline-injected animals.

At one month after injections, the scaffold made of B24 did not exert any chronic inflammation in the spinal cord: on the contrary, it has been widely invaded by regenerating nervous fibers (figure 8a) positive to βIIITubulin and GAP-43 neuronal markers. In particular, bundles of newly formed axons infiltrated the inner portion of the implanted scaffold (figure 8b).

Taken together these results evince an appreciable *in vivo* biocompatibility of the

tested peptides, and their potential as scaffolds for nervous regenerative applications.

The novel self-assembling peptides according to the present invention and made according to Examples 1-7 form tabular nanofibres which surprisingly self assemble into complex interwoven membranes of a few microns in width in mild conditions. Interestingly such novel peptides also have self-healing properties and can be used for different applications such as scaffolds for in vitro cell culture and tissue regeneration, drug delivery, hemostatic compounds and other non-medical applications such as molecular switches and pH sensitive devices.

From the above description and the above-noted Examples, the advantages attained by the product described and obtained according to the present invention are apparent.

References

1. Tibbitt, M.W. & Anseth, K.S. Hydrogels as extracellular matrix mimics for 3D cell culture. Biotechnol Bioeng 103, 655-663 (2009).
2. Hamidi, M., Azadi, A. & Rafiei, P. Hydrogel nanoparticles in drug delivery. Adv Drug Deliv Rev60, 1638-1649 (2008).
3. Nisbet, D.R., Crompton, K.E., Horne, M.K., Finkelstein, D.I. & Forsythe, J.S. Neural tissue engineering of the CNS using hydrogels. J Biomed Mater Res B Appl Biomater87, 251-263 (2008).
4. Kisiday, J. et al. Self-assembling peptide hydrogel fosters chondrocyte extracellular matrix production and cell division: implications for cartilage tissue repair. Proc Natl Acad Sci U S A99, 9996-10001 (2002).
5. Gelain, F., Bottai, D., Vescovi, A. & Zhang, S. Designer self-assembling Peptide nanofiber scaffolds for adult mouse neural stem cell 3-dimensional cultures. PLoS ONE1, e119 (2006).
6. Zhang, S., Gelain, F. & Zhao, X. Designer self-assembling peptide nanofiber scaffolds for 3D tissue cell cultures. Semin Cancer Biol15, 413-420 (2005).
7. Zhang, S., Holmes, T., Lockshin, C. & Rich, A. Spontaneous assembly of a self-complementary oligopeptide to form a stable macroscopic membrane. Proc Natl Acad Sci U S A90, 3334-3338 (1993).
8. Gazit, E. Self-assembled peptide nanostructures: the design of molecular building blocks and their technological utilization. Chem Soc Rev36, 1263-1269 (2007).
9. Taraballi, F. et al. Effect of functionalization on the self-assembling propensity of beta-sheet forming peptides. Soft Matter5, 660-668 (2009).
10. Jitrapakdee, S. & Wallace, J.C. The biotin enzyme family: conserved structural motifs and domain rearrangements. Curr Protein Pept Sci4, 217-229 (2003).
11. Lei, Y., Li, H., Zhang, R. & Han, S. Theoretical study of cooperativity in biotin. J Phys Chem B111, 14370-14377 (2007).
12. Zuckermann, R.N. & Kodadek, T. Peptoids as potential therapeutics. Curr Opin Mol Ther11, 299-307 (2009).

13. D'Souza, S.E., Ginsberg, M.H. & Plow, E.F. Arginyl-glycyl-aspartic acid (RGD): a cell adhesion motif. Trends Biochem Sci16, 246-250 (1991).

14. Reches, M. & Gazit, E. Casting metal nanowires within discrete self-assembled peptide nanotubes. Science (New York, N.Y300, 625-627 (2003).

15. Vescovi, A.L., Reynolds, B.A., Fraser, D.D. & Weiss, S. bFGF regulates the proliferative fate of unipotent (neuronal) and bipotent (neuronal/astroglial) EGF-generated CNS progenitor cells. Neuron11, 951-966 (1993).

16. Vescovi, A.L. et al. Isolation and cloning of multipotential stem cells from the embryonic human CNS and establishment of transplantable human neural stem cell lines by epigenetic stimulation. Exp Neurol156, 71-83 (1999).

CLAIMS

1. A self-assembling peptide (SAP) consisting of an amino acid domain,

- having from 7 to 17 aminoacids, said domain being:

-GGGPFSSTKT-	SEQ ID N.1
-WGGGPFSSTKT-	SEQ ID N.2
-GGGPFSSTDT-	SEQ ID N.3
-GGGPFSSTNT-	SEQ ID N.4
-GGGPFSSTET-	SEQ ID N.5
-GGGPFSSTQT-	SEQ ID N.6
-GGGAFSSTKT-	SEQ ID N.7
-GGGPFSETKT-	SEQ ID N.8
-GGGAFSSTKTGRGD-	SEQ ID N.9
-GGGPFSSTRT-	SEQ ID N.10
-GGGAFASTKT-	SEQ ID N.11
-GGGGGPFSSTKT-	SEQ ID N.12
-GGGPWSSTKT-	SEQ ID N.13
-GGG(Propylamine)FSSTKT-	SEQ ID N.14
-WGGGAFASTKT-	SEQ ID N.15
-WGGGAFSSTKT-	SEQ ID N.16
-GGGKFSSTPT-	SEQ ID N.17
-GGGPKSSTFT-	SEQ ID N.18
-GGGPFSSKTT-	SEQ ID N.19
-GGGPFSSTTK-	SEQ ID N.20
-GGGGPFSSTKT-	SEQ ID N.21
--GGGPFSSTKTGRGD-	SEQ ID N.22
-GPFSSTKT-	SEQ ID N.23
-GGGAWASTKT-	SEQ ID N.24
-GGGAFASTKA-	SEQ ID N.25
-GGGPFSSTKTP	SEQ ID N.26
-FGGGPFSSTKT-	SEQ ID N.27
-GGGPYSSTKT-	SEQ ID N.28
-GGGAASSTKT-	SEQ ID N.29

-GGGAFAATKT-	SEQ ID N.30
-GGGAFASAKA-	SEQ ID N.31
-GGGPFSSTAT-	SEQ ID N.32
-GGGAFAAAKA-	SEQ ID N.33
-GGGPFSSAKT-	SEQ ID N.34
-GGGPFSATKT-	SEQ ID N.35
-GGGPFSCTKT-	SEQ ID N.36
-GGGPFCSTKT-	SEQ ID N.37
-GAFASTKT-	SEQ ID N.38
-GGGGGAFASTKT-	SEQ ID N.39
-GGGAFASTKTGRGD-	SEQ ID N.40
-GGGPFSSTKTGIKVAV-	SEQ ID N.41
-GGGAFASTKTGIKVAV-	SEQ ID N.42
-GGGAFAK-	SEQ ID N.43
-$(GGG)_2$-KFSSTKT-	SEQ ID N.44
-FGGGAFASTKTGIKVAV-	SEQ ID N.45
-YGGGPFSSTKT-	SEQ ID N.46; or
-FGGGAFSSTKT-	SEQ ID N.47.

2. The self-assembling peptide according to claim 1 and having an amino acid domain selected from the group consisting of SEQ ID NO. 1, 3, 4, 5, 6, 7, 8, 9, 10, 11, 12, 13, 14, 17, 18, 19, 20, 21, 22, 40, 41, 42, 44 and 45.

3. The self-assembling peptide according to claim 1 and having an amino acid domain selected from the group consisting of SEQ ID NO. 1, 8, 10 and 13.

4. The self-assembling peptide according to claim 2 and having the amino acid domain consisting of SEQ ID NO. 14, wherein a propylamine is present between the G in position 3 and the F in position 4.

5. The self-assembling peptide according to claim 2 and having the amino acid domain consisting of SEQ ID NO.11

6. The self-assembling peptide according to anyone of claims 2 to 5 wherein the N-terminus is optionally biotinylated.

7. The self-assembling peptide according to claim 1 and having an amino acid

domain selected from the group consisting of SEQ ID NO. 2, 15 and 16.

8. The self-assembling peptide according to claim 7 wherein the N-terminus is optionally acetylated.

9. The self-assembling peptide according to anyone of claims 1 to 8, wherein the number of Glycines of the aminoacid domain is of 1 to 8.

10. The self-assembling peptide according to claims 9, wherein the number of Glycines of the aminoacid domain is of 3 to 6.

11. Hydrogel comprising the self-assembling peptides according to claims 1 to 10 and a hydrogelating ingredient.

12. A self-assembling peptide polymer comprising at least 2 identical self-assembling peptides according to anyone of claims 1 to 10.

13. A self-assembling peptide polymer comprising at least 2 different self-assembling peptides according to anyone of claims 1 to 10

14. Use of the self-assembling peptide polymer according to claims 12 or 13 as a medicament.

15. A tabular nanofiber comprising at least 2 identical self-assembling peptides according to anyone of claims 1 to 10.

16. A tabular nanofiber comprising at least 2 different self-assembling peptides according to anyone of claims 1 to 10.

17. A tabular nanofiber according to claims 15 or 16, characterised in that it is from 5 to 10μm in length.

18. A complex interwoven membrane made of at least 2 tabular nanofibres according to anyone of claims 15, 16 or 17.

19. A complex interwoven membrane according to claim 18, characterised in that it is 0.5 - 4 μm wide.

20. A self-assembled nanostructure consisting of 2 or more identical peptides according to claims 1 to 10.

21. A self-assembled nanostructure consisting of 2 or more different peptides according to claims 1 to 10

22. The self-assembled nanostructure according to claims 20 or 21 having a hollow cavity.

23. Use of a self-assembled nanostructure according to claims 20, 21 or 22 for the

release of molecular drugs.

24. A pharmaceutical composition comprising at least one polymer according to claim 12 and a pharmaceutically bioactive excipient.

25. Use of the hydrogel according to claim 11 as a scaffold for in vitro cell culture.

26. Use of the hydrogel according to claim 11 for in vitro cell culture in 2 and 3 dimensions.

27. Use of the hydrogel according to claim 11 as a scaffold for the in vitro growth and differentiation of human neural stem cells.

28. Use of the hydrogel according to claim 11 as a scaffold for the in vitro growth and differentiation of murine neural stem cells

29. Use of the hydrogel according to claim 11 for in vivo nervous regeneration.

30. Use of the hydrogel according to claim 11 for hemostasis.

31. Use of the hydrogel according to claim 11 as a device for in vivo drug delivery.

32. Use of the hydrogel according to claim 11 for tissue engineering.

33. Use of the hydrogel according to claim 11 as a molecular switch or as a biosensor.

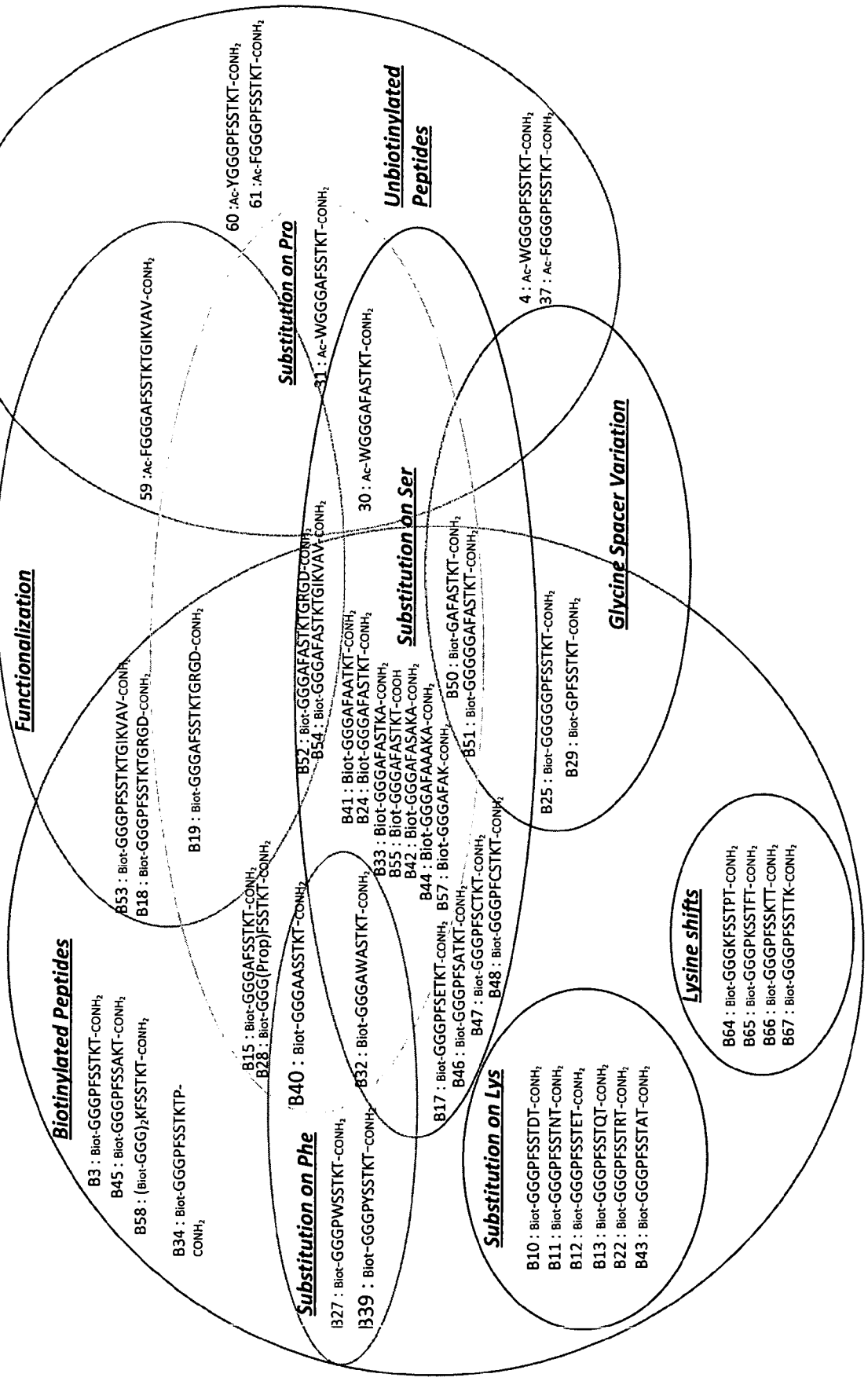
Functionalization
Biotinylated Peptides
B3 : Biot-GGGPFSSTKT-CONH2
B45 : Biot-GGGPFSSAKT-CONH2
B58 : (Biot-GGG)2KFSSTKT-CONH2
B34 : Biot-GGGPFSSTKTP-CONH2
B53 : Biot-GGGPFSSTKTGIKVAV-CONH2
B18 : Biot-GGGPFSSTKTGRGD-CONH2
B19 : Biot-GGGAFSSTKTGRGD-CONH2
59 :Ac-FGGGAFSSTKTGIKVAV-CONH2
60 :Ac-YGGGPFSSTKT-CONH2
61 :Ac-FGGGPFSSTKT-CONH2
Substitution on Pro
B52 : Biot-GGGAFASTKTGRGD-CONH2
B54 : Biot-GGGAFASTKTGIKVAV-CONH2
31 : Ac-WGGGAFSSTKT-CONH2
Unbiotinylated Peptides
Substitution on Ser
B41 : Biot-GGGAFAATKT-CONH2
B24 : Biot-GGGAFASTKT-CONH2
B33 : Biot-GGGAFASTKA-CONH2
B55 : Biot-GGGAFASTKT-COOH
B42 : Biot-GGGAFASAKA-CONH2
B44 : Biot-GGGAFAAAKA-CONH2
30 : Ac-WGGGAFASTKT-CONH2
B15 : Biot-GGGAFSSTKT-CONH2
B28 : Biot-GGG(Prop)FSSTKT-CONH2
B40 : Biot-GGGAASSTKT-CONH2
Substitution on Phe
B27 : Biot-GGGPWSSTKT-CONH2
B39 : Biot-GGGPYSSTKT-CONH2
B32 : Biot-GGGAWASTKT-CONH2
B17 : Biot-GGGPFSETKT-CONH2
B46 : Biot-GGGPFSATKT-CONH2
B57 : Biot-GGGAFAK-CONH2
B47 : Biot-GGGPFSCTKT-CONH2
B48 : Biot-GGGPFCSTKT-CONH2
B50 : Biot-GAFASTKT-CONH2
B51 : Biot-GGGGGAFASTKT-CONH2
4 : Ac-WGGGPFSSTKT-CONH2
37 : Ac-FGGGPFSSTKT-CONH2
Glycine Spacer Variation
B25 : Biot-GGGGGPFSSTKT-CONH2
B29 : Biot-GPFSSTKT-CONH2
Substitution on Lys
B10 : Biot-GGGPFSSTDT-CONH2
B11 : Biot-GGGPFSSTNT-CONH2
B12 : Biot-GGGPFSSTET-CONH2
B13 : Biot-GGGPFSSTQT-CONH2
B22 : Biot-GGGPFSSTRT-CONH2
B43 : Biot-GGGPFSSTAT-CONH2
Lysine shifts
B64 : Biot-GGGKFSSTPT-CONH2
B65 : Biot-GGGPKSSTFT-CONH2
B66 : Biot-GGGPFSSKTT-CONH2
B67 : Biot-GGGPFSSTTK-CONH2

Figure 1

Figure 2a

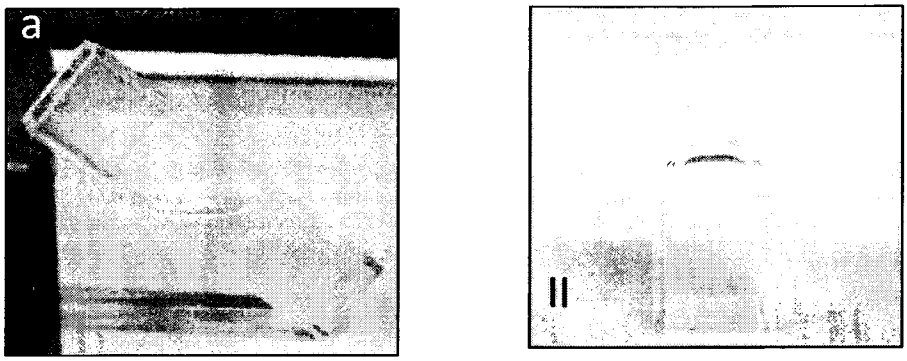

Figure 2b

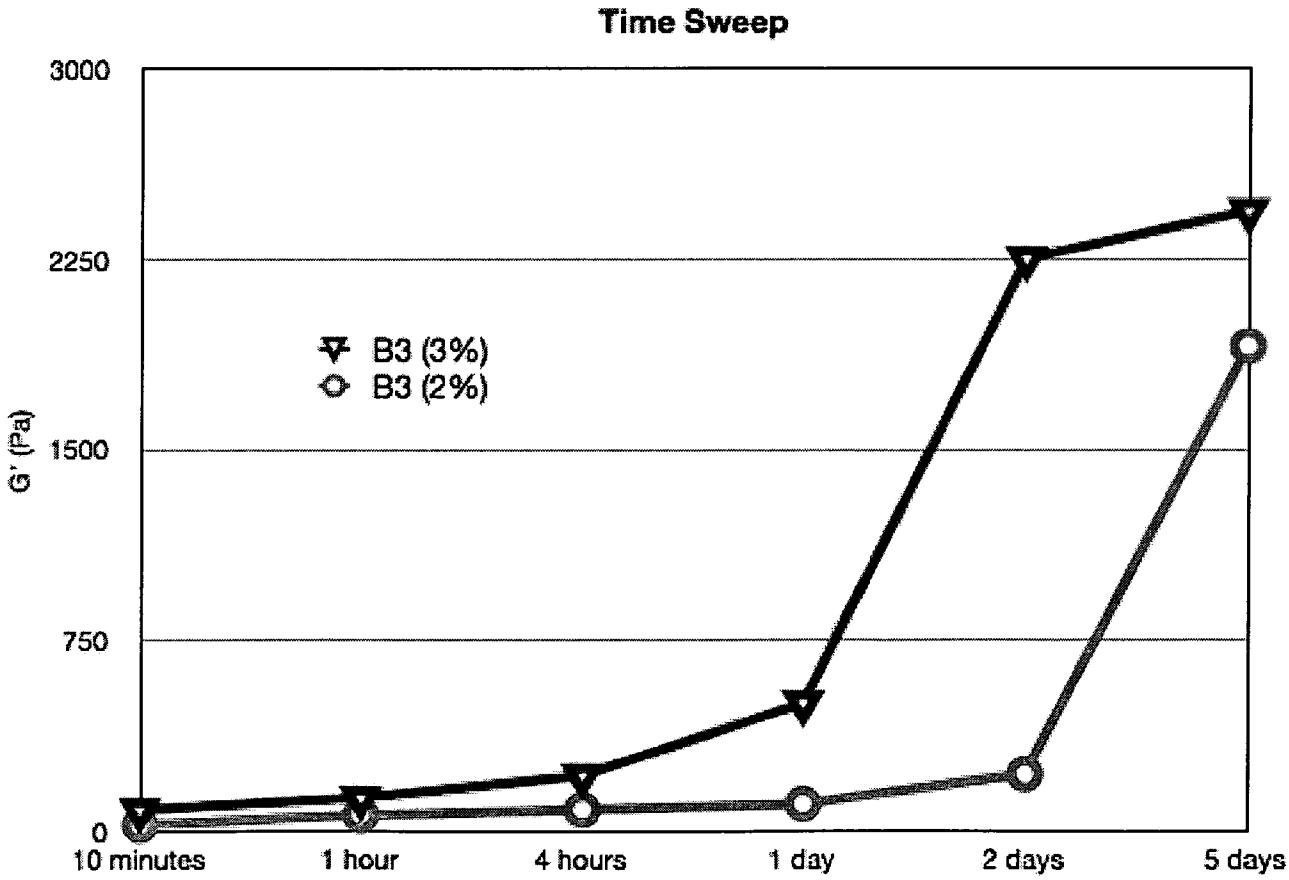

Figure 2c

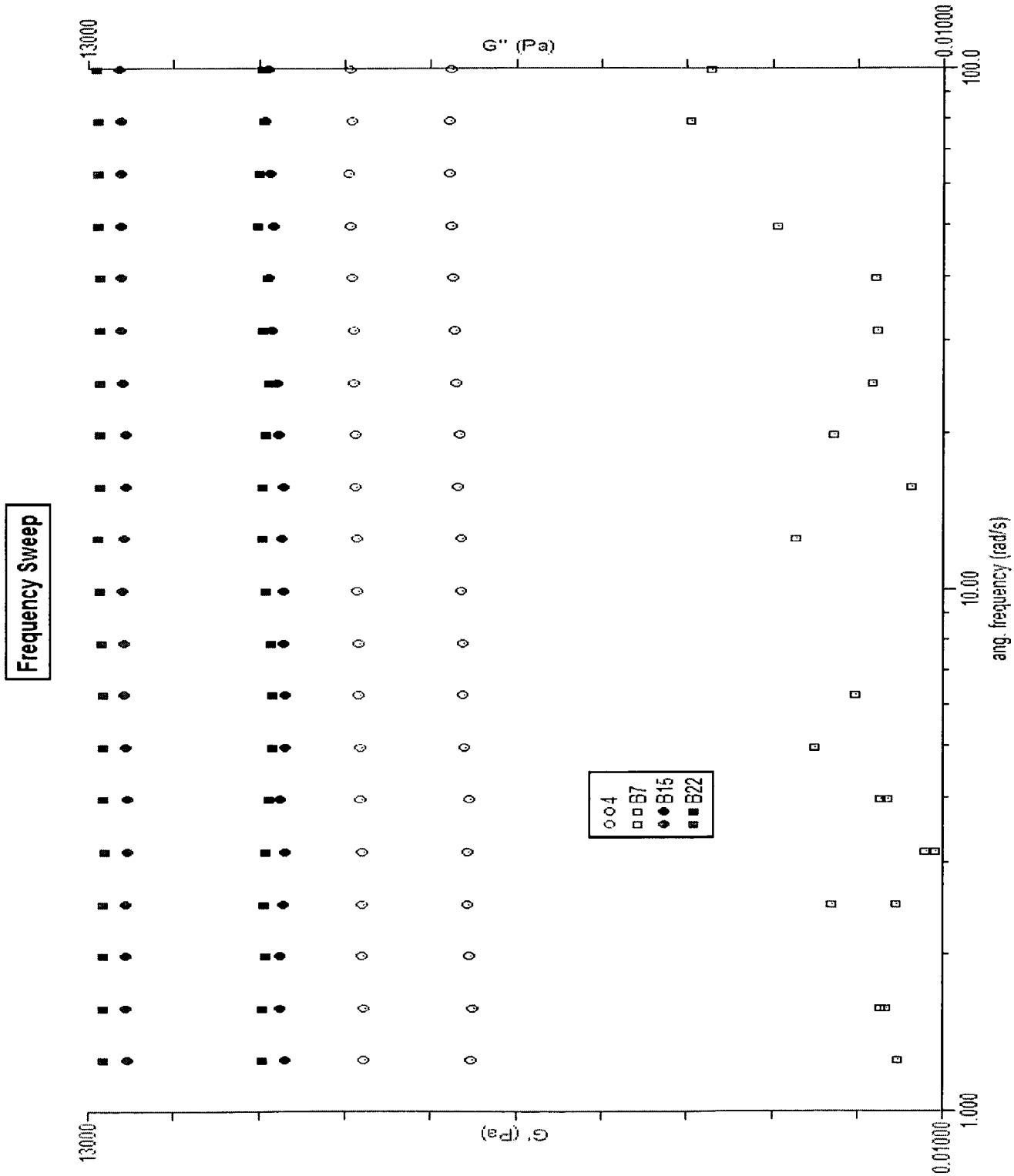
Frequency Sweep
G'' (Pa)
G' (Pa)
13000
13000
0.01000
100.0
10.00
1.000
0.01000
ang. frequency (rad/s)
04
B7
B15
B22

Figure 2 d

Peptide identification numbers	Peptide sequences	G' pre-assembling	G' post-assembling
B3 * (SEQ ID NO. 1)	Biot-GGGPFSSTKT-CONH2	67 Pa	2917 Pa
4 " (SEQ ID NO. 2)	Ac-WGGGPFSSTKT-CONH2	0.05 Pa	158 Pa
B10 (SEQ ID NO. 3)	Biot-GGGPFSSTDT-CONH2	Immediate Gelation	Immediate Gelation
B11 (SEQ ID NO.4)	Biot-GGGPFSSTNT-CONH2	Immediate Gelation	Immediate Gelation
B12 (SEQ ID NO.5)	Biot-GGGPFSSTET-CONH2	Immediate Gelation	Immediate Gelation
B13 (SEQ ID NO. 6)	Biot-GGGPFSSTQT-CONH2	Immediate Gelation	Immediate Gelation
B15 (SEQ ID NO. 7)	Biot-GGGAFSSTKT-CONH2	18 Pa	8500 Pa
B17 (SEQ ID NO. 8)	Biot-GGGPFSETKT-CONH2	2.12Pa	1615 Pa
B19 ** (SEQ ID NO.9)	Biot-GGGAFSSTKTGRGD-CONH2	0.144 Pa	114.7 Pa
B22 * (SEQ ID NO. 10)	Biot-GGGPFSSTRT-CONH2	58.68 Pa	8715 Pa
B24 * (SEQ ID NO. 11)	Biot-GGGAFASTKT-CONH2	2.72 Pa	6502 Pa
B25 (SEQ ID NO. 12)	Biot-GGGGGPFSSTKT-CONH2	3.08 Pa	403.5 Pa
B27 " (SEQ ID NO.13)	Biot-GGGPWSSTKT-CONH2	22.3 Pa	8566
B28 ^ (SEQ ID NO.14)	Biot-GGG(Propylamine)FSSTKT-CONH2	0.2628 Pa	687.2 Pa
30 "** (SEQ ID NO.15)	Ac-WGGGAFASTKT-CONH2	0.55 Pa	101 Pa
31 ** (SEQ ID NO.16)	Ac-WGGGAFSSTKT-CONH2	4.02 Pa	5337 Pa
1 (SEQ ID NO.22)	Ac-PFSSTKT-CONH2	N.G.	No Gelation
2 (SEQ ID NO.23)	Ac-GGGPFSSTKT-CONH2	<0.001 Pa	No Gelation

Figure 3 a

B64	Biot-GGGKFSSTPT-CONH2
B65	Biot-GGGPKSSTFT-CONH2
B66	Biot-GGGPFSSKTT-CONH2
B67	Biot-GGGPFSSTTK-CONH2

Figure 3 b

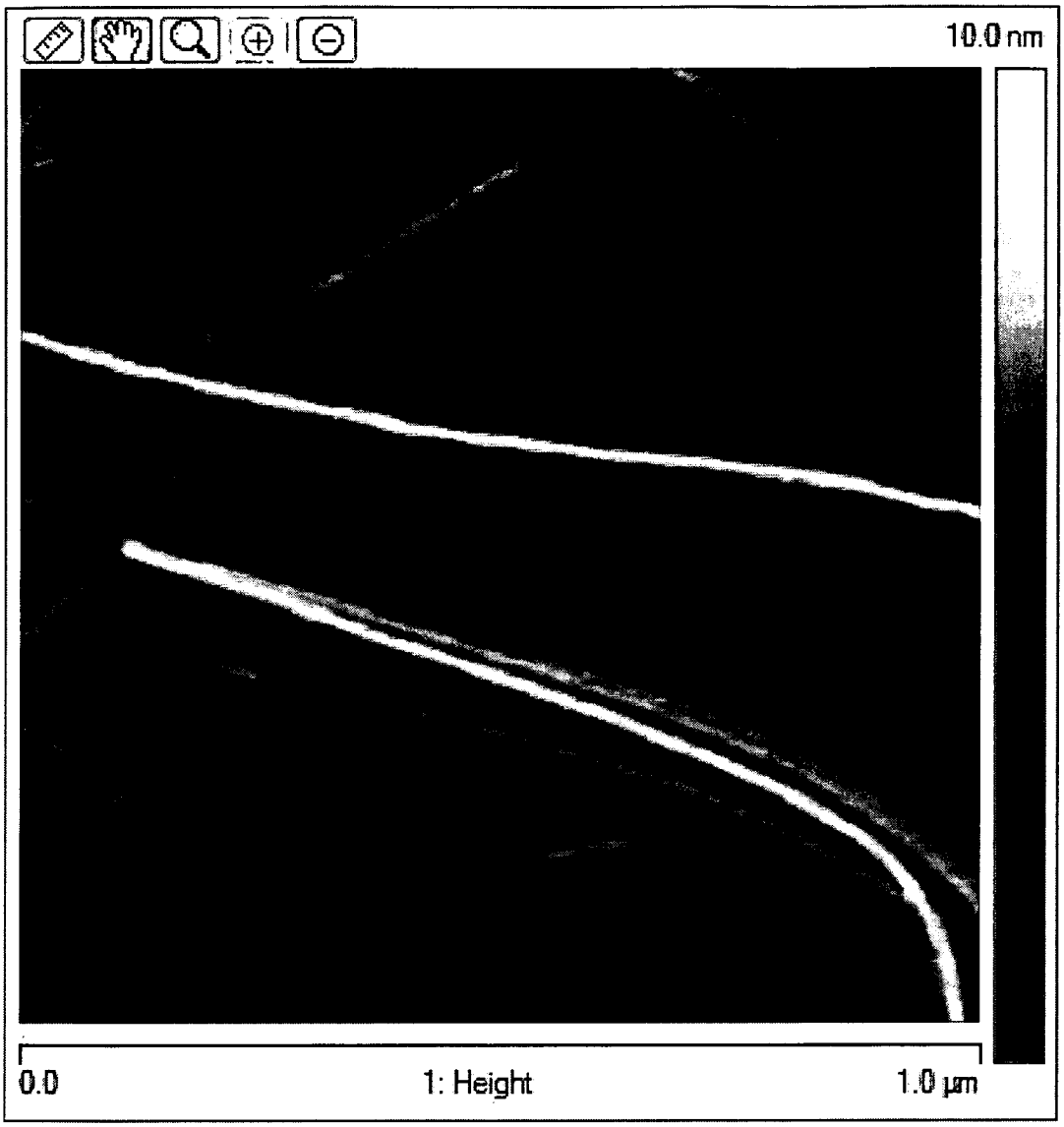

B32	Biot-GGGAWASTKT-CONH2
B33	Biot-GGGAFASTKA-CONH2
B40	Biot-GGGAASSTKT-CONH2
B41	Biot-GGGAFAATKT-CONH2
B42	Biot-GGGAFASAKA-CONH2
B15	Biot-GGGAFSSTKT-CONH2
B24	Biot-GGGAFASTKT-CONH2
B54	Biot-GGGAFASTKTGIKVAV-CONH2
B58	(Biot-GGG)2KFSSTKT-CONH2
59	Ac-FGGGAFASTKTGIKVAV-CONH2
B44	Biot-GGGAFAAAKA-CONH2
61	Ac-FGGGAFSSTKT-CONH2

Figure 3 c

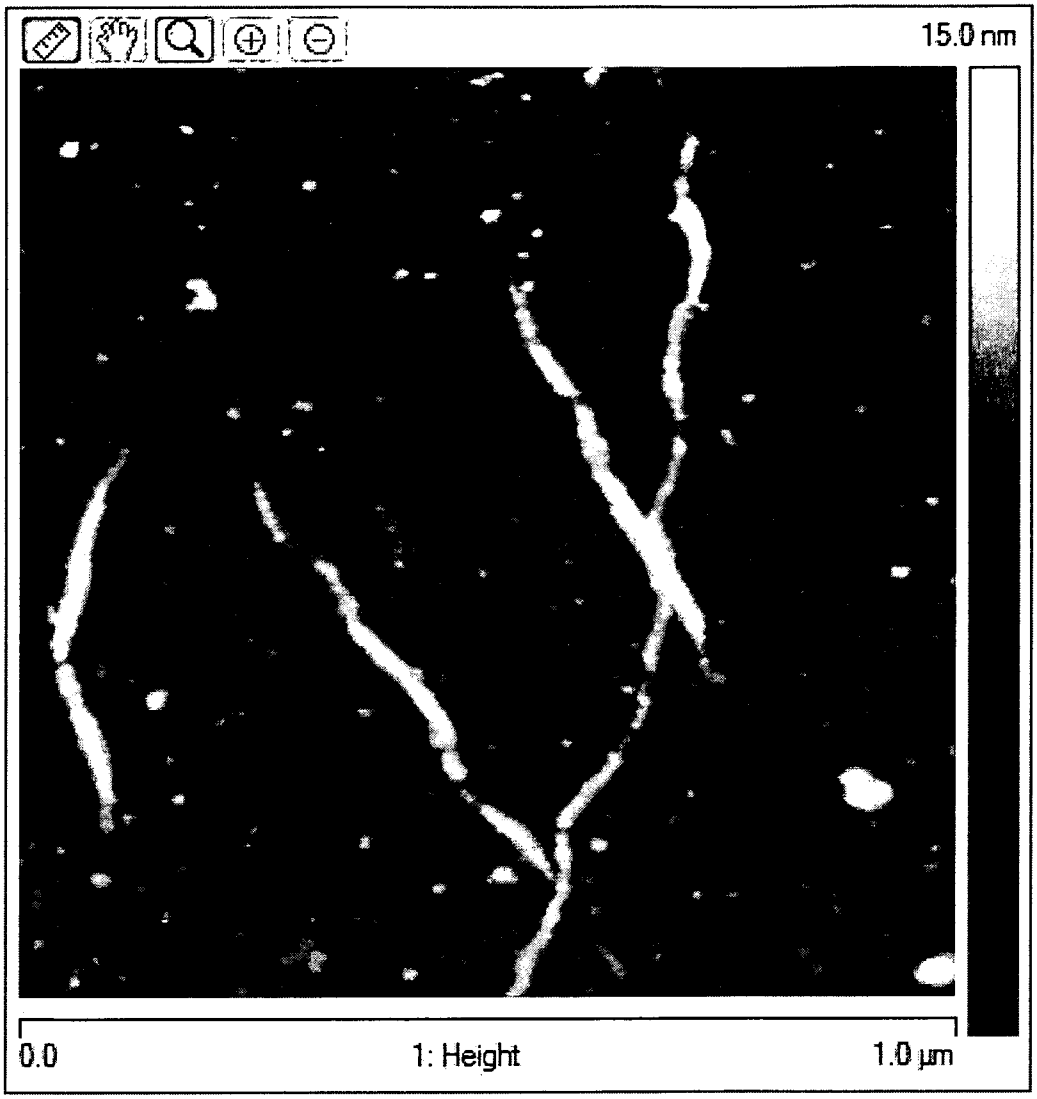

4	Ac-WGGGPFSSTKT-CONH2
37	Ac-FGGGPFSSTKT-CONH2
60	Ac-YGGGPFSSTKT-CONH2

Figure 3 d

B10	Biot-GGGPFSSTDT-CONH2
B11	Biot-GGGPFSSTNT-CONH2
B12	Biot-GGGPFSSTET-CONH2
B13	Biot-GGGPFSSTQT-CONH2
B43	Biot-GGGPFSSTAT-CONH2

Figure 3 e

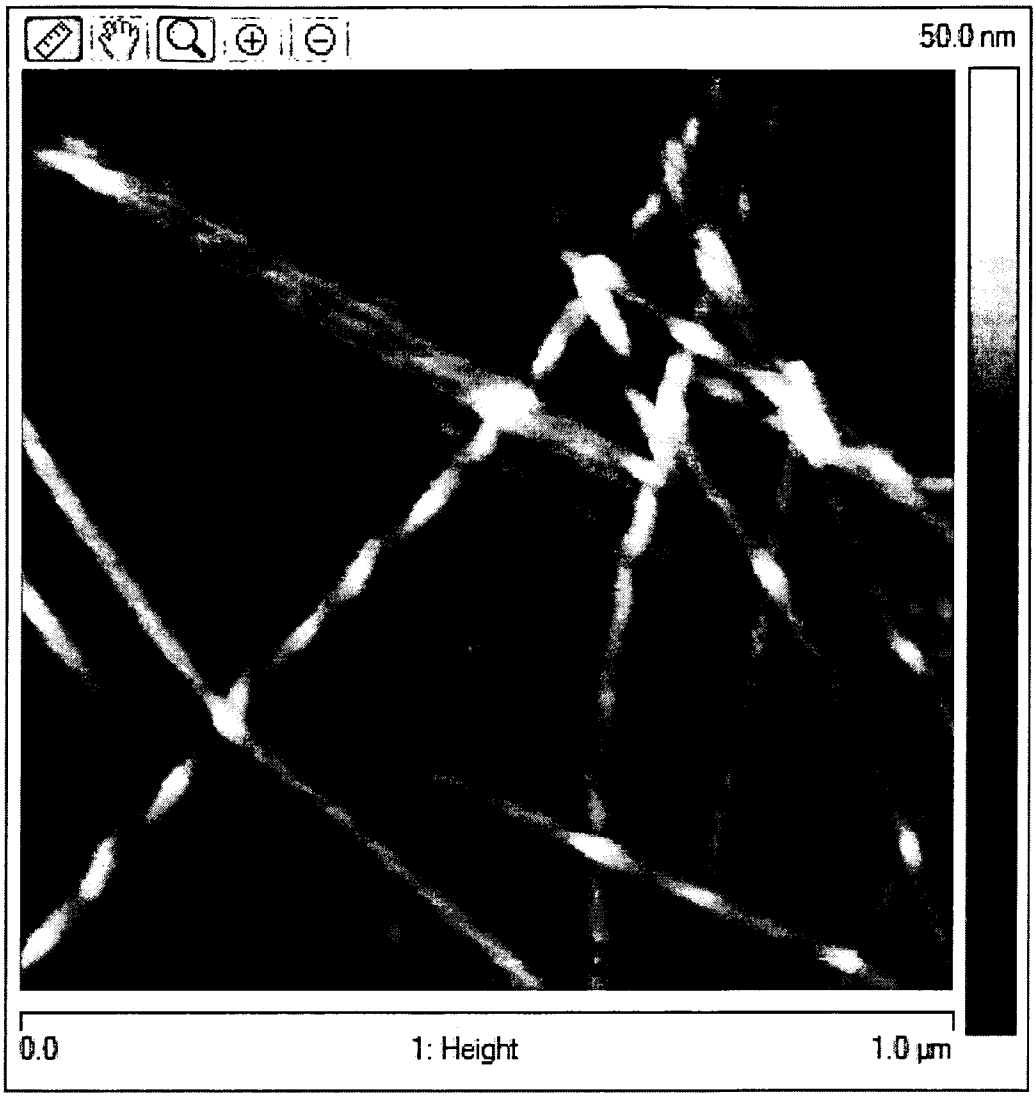

B53	Biot-GGGPFSSTKTGIKVAV-CONH2
B50	Biot-GAFASTKT-CONH2
B18	Biot-GGGPFSSTKTGRGD-CONH2
B19	Biot-GGGAFSSTKTGRGD-CONH2
B25	Biot-GGGGGPFSSTKT-CONH2
B28	Biot-GGG(Propylamine)FSSTKT-CONH2
B29	Biot-GPFSSTKT-CONH2
30	Ac-WGGGAFASTKT-CONH2
31	Ac-WGGGAFSSTKT-CONH2
B45	Biot-GGGPFSSAKT-CONH2
B52	Biot-GGGAFASTKTGRGD-CONH2
B51	Biot-GGGGGAFASTKT-CONH2

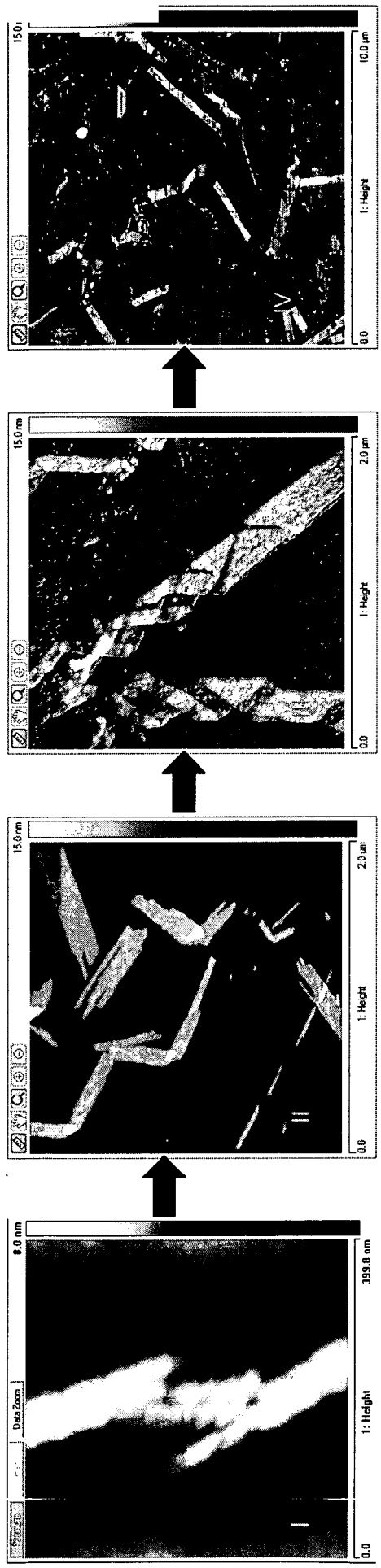

Figure 3 f

B3 Biot-GGGPFSSTKT-CONH2
B17 Biot-GGGPFSETKT-CONH2
B22 Biot-GGGPFSSTRT-CONH2
B27 Biot-GGGPWSSTKT-CONH2
B34 Biot-GGGPFSSTKTP-CONH2
B39 Biot-GGGPYSSTKTP-CONH2
B46 Biot-GGGPFSATKT-CONH2
B47 Biot-GGGPFSCTKT-CONH2
B48 Biot-GGGPFCSTKT-CONH2
B57 Biot-GGGAFAK-CONH2

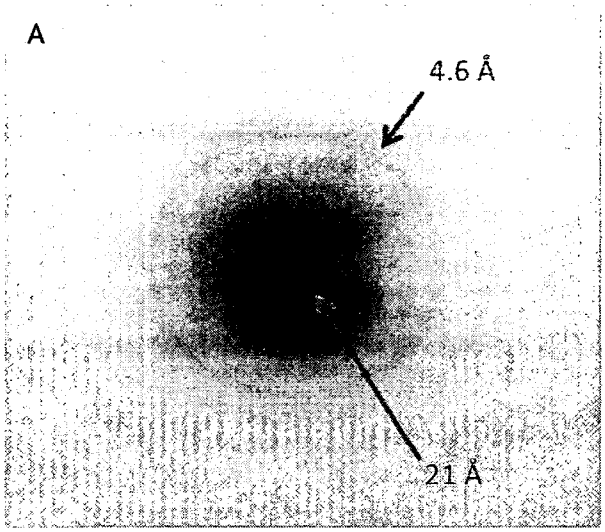

Figure 4 a

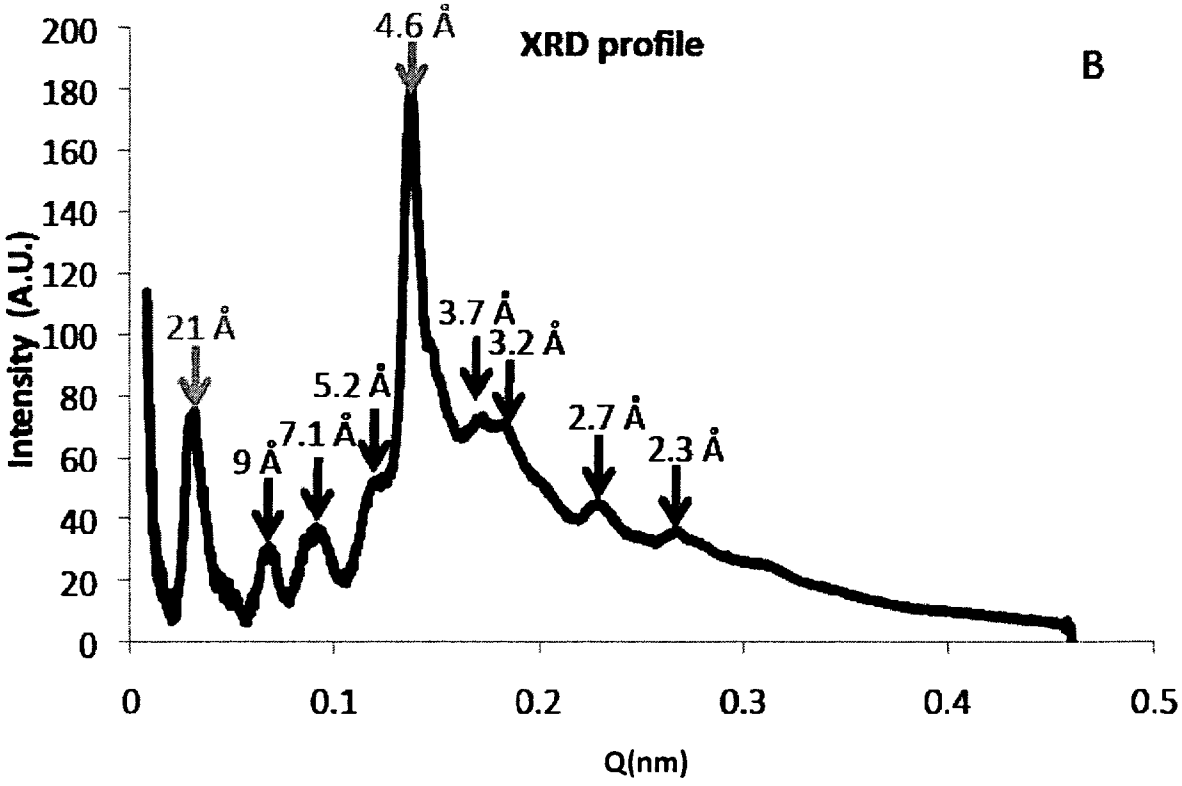

Figure 4 b

Diffraction maxima of the tested peptides					
Peptide	d, Å	intensity	Peptide	d, Å	intensity
B3	21.00	s	B25	19.60	w
	9.00	m		12.00	w
	7.10	m		8.00	vw
	5.20	w		6.60	vw
	4.60	vs		4.60	vs
	3.70	w		3.80	m
	3.20	w		3.00	w
	2.70	w		2.40	w
	2.30	vw	B33	16.90	w
4	23.50	s		8.50	vw
	11.70	w		6.50	vw
	4.60	s		4.60	vs
	3.80	w		4.00	w
	2.38	vw		3.70	m
B12	20.50	m		2.90	vw
	9.50	w		2.40	vw
	7.00	w	B34	21.0	m
	4.60	vs		7.10	w
	4.30	vs		5.30	w
	3.81	m		4.60	vs
	2.34	vw		3.70	w
B13	21.90	s	B47	21.50	m
	17.30	s		17.10	m
	12.00	w		9.10	w
	10.10	w		7.10	m
	8.70	w		4.60	vs
	7.10	m		4.30	s
	5.09	w		3.70	w
	4.60	vs		3.20	vw
	3.60	m		2.80	vw
	3.20	w		2.50	vw
	2.70	w		2.30	vw
	2.30	vw	B48	17.50	vw
B15	17.30	m		5.50	vw
	7.70	w		4.60	s
	4.60	vs		4.00	m
	4.16	w		3.70	vw
	3.70	m		2.30	vw
	3.40	vw	B53	20.82	vw
	2.30	vw		9.7	w
B19	28.60	m		7.50	w
	8.10	w		4.60	vs
	4.64	vs		3.70	m
	4.08	m		3.10	vw
	3.85	w		2.80	vw
	2.40	vw		2.30	vw

Figure 4 c

vs, very strong; s,strong; m, medium; w,weak; vw, very weak

Figure 4 d

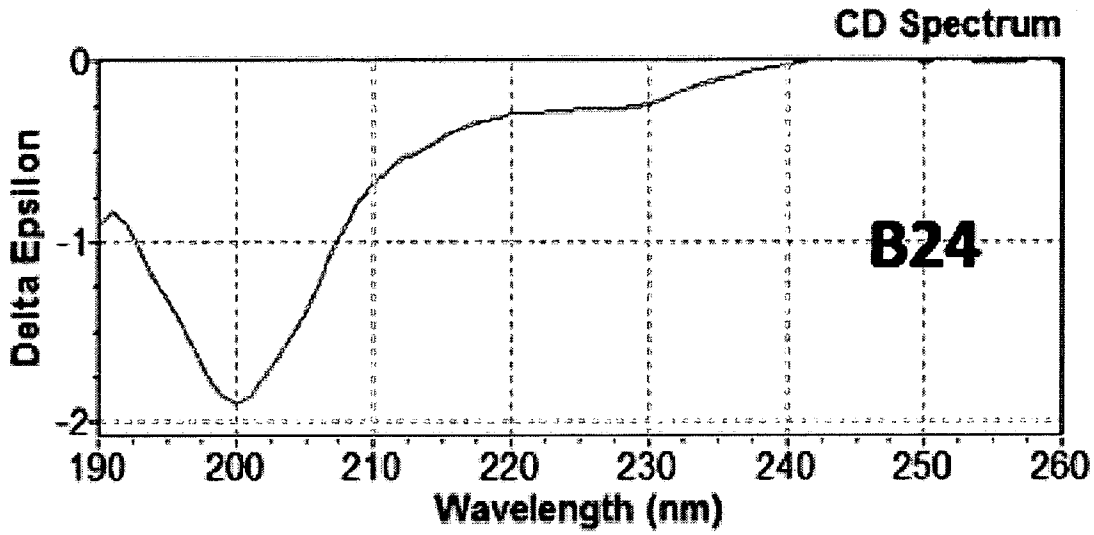
CD Spectrum
Delta Epsilon
0
-1
-2
B24
190
200
210
220
230
240
250
260
Wavelength (nm)

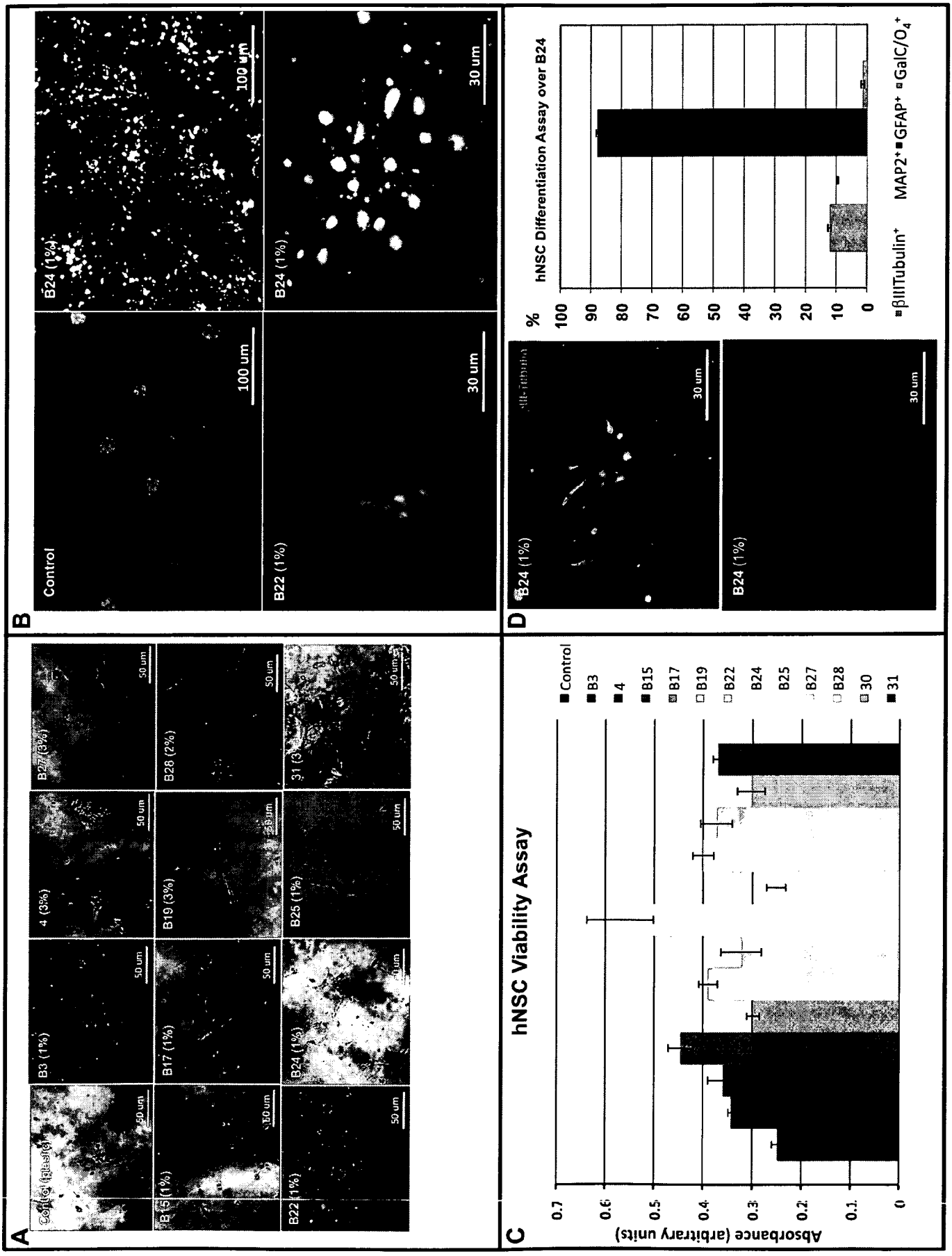
A
Control (plain)
B3 (1%)
4 (3%)
B27 (3%)
B15 (1%)
B17 (1%)
B19 (3%)
B28 (2%)
B22 (1%)
B24 (1%)
B25 (1%)
31 (3%)
50 um
B
Control
B22 (1%)
B24 (1%)
100 um
30 um
C
hNSC Viability Assay
Absorbance (arbitrary units)
0
0.1
0.2
0.3
0.4
0.5
0.6
0.7
Control
B3
4
B15
B17
B19
B22
B24
B25
B27
B28
30
31
D
B24 (1%)
hNSC Differentiation Assay over B24
%
0
10
20
30
40
50
60
70
80
90
100
βIIITubulin+
MAP2+
GFAP+
GalC/O4+

Figure 5

Figure 6 a

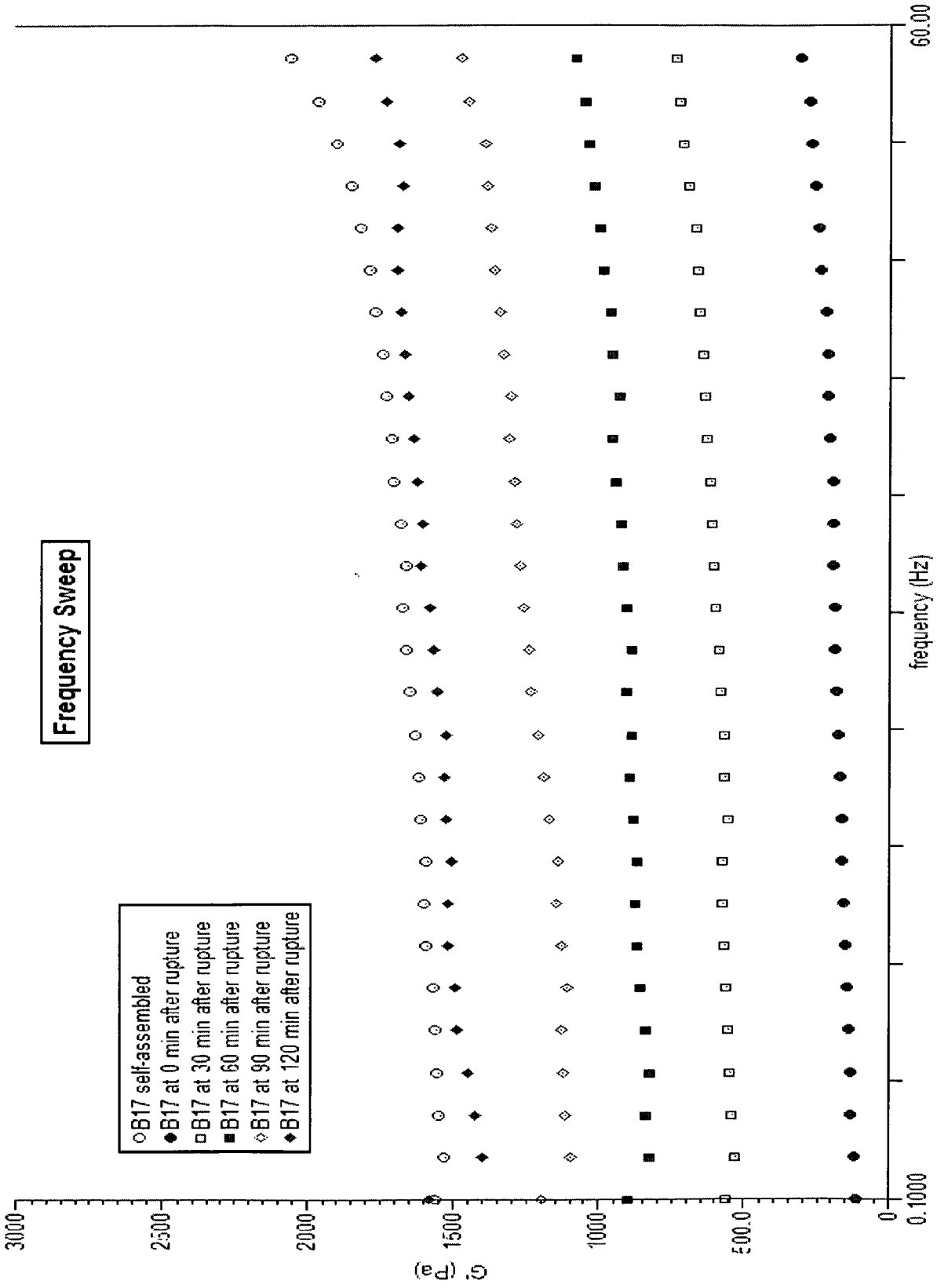
Frequency Sweep
B17 self-assembled
B17 at 0 min after rupture
B17 at 30 min after rupture
B17 at 60 min after rupture
B17 at 90 min after rupture
B17 at 120 min after rupture
G' (Pa)
3000
2500
2000
1500
1000
500.0
0
0.1000
60.00
frequency (Hz)

Figure 6 b

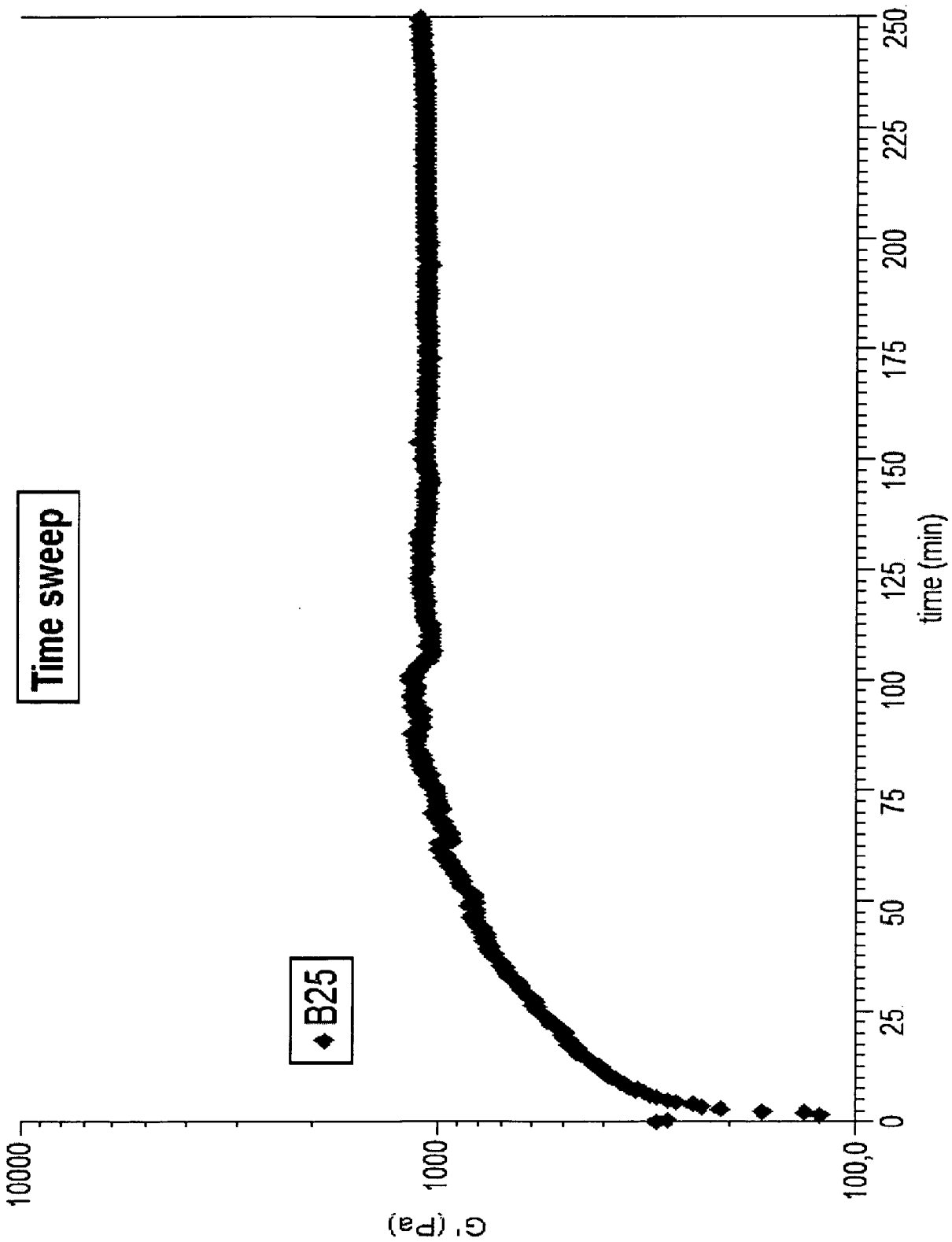
Time sweep
B25
G' (Pa)
10000
1000
100,0
0
25
50
75
100
125
150
175
200
225
250
time (min)

Figure 6 c

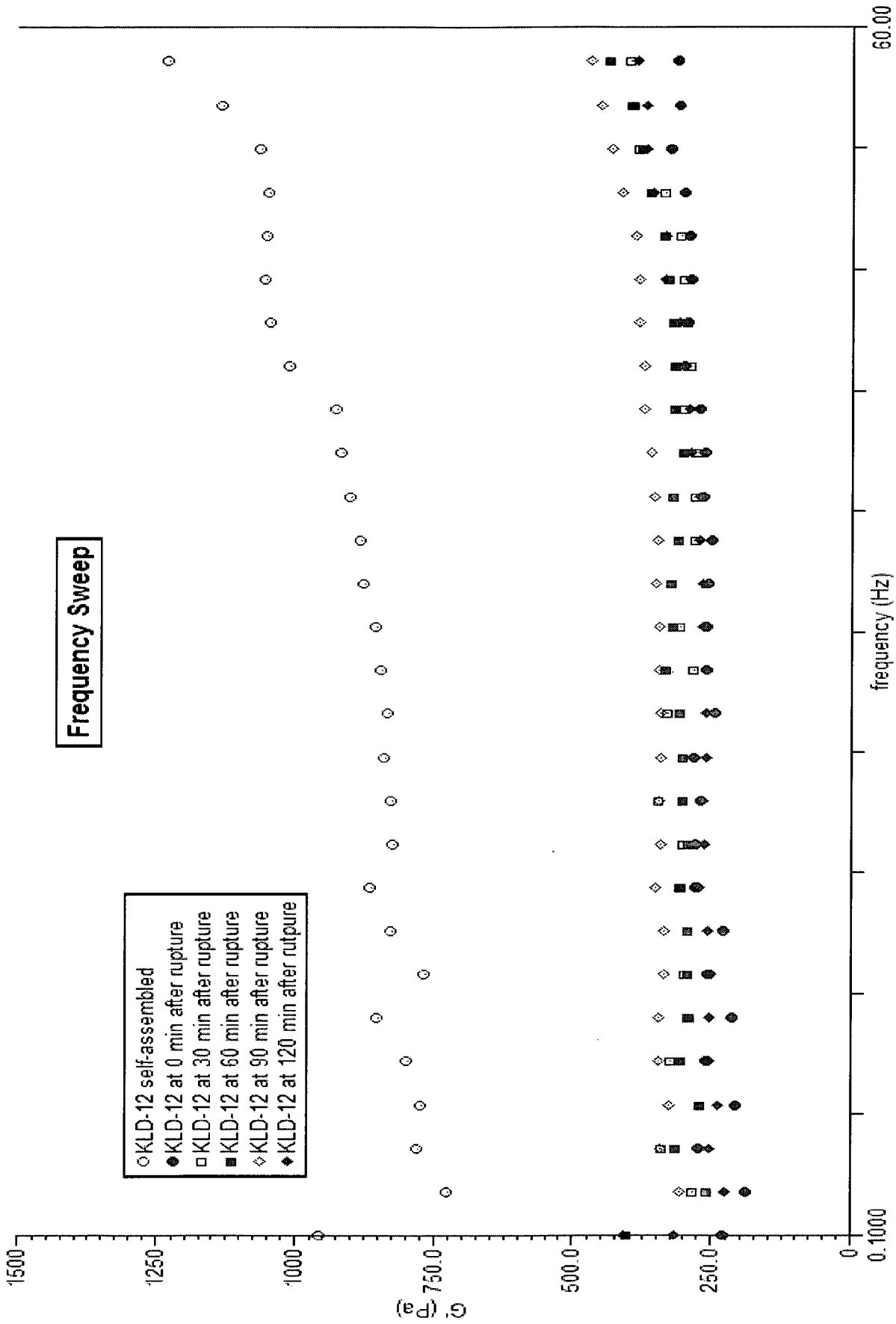
Frequency Sweep
KLD-12 self-assembled
KLD-12 at 0 min after rupture
KLD-12 at 30 min after rupture
KLD-12 at 60 min after rupture
KLD-12 at 90 min after rupture
KLD-12 at 120 min after rutpure
G' (Pa)
1500
1250
1000
750.0
500.0
250.0
0
0.1000
60.00
frequency (Hz)

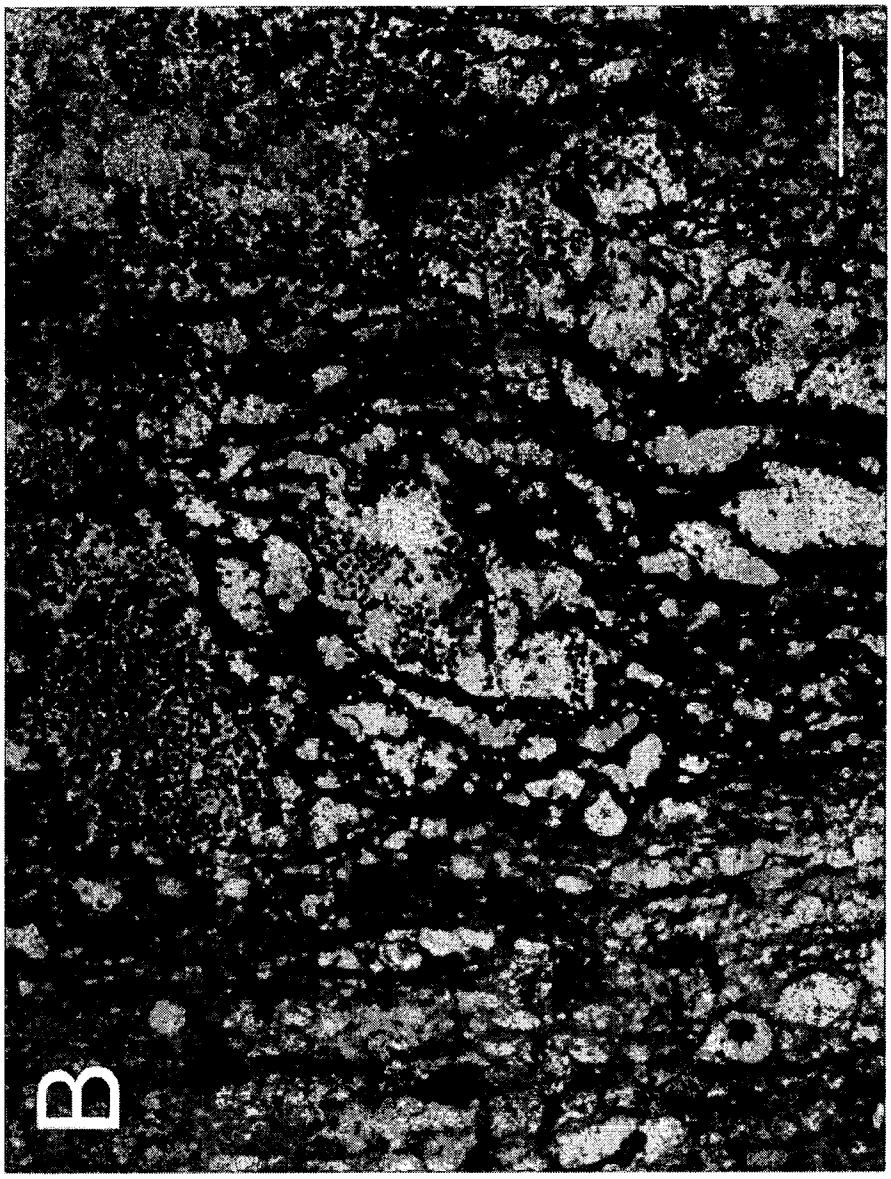

Figure 7 b

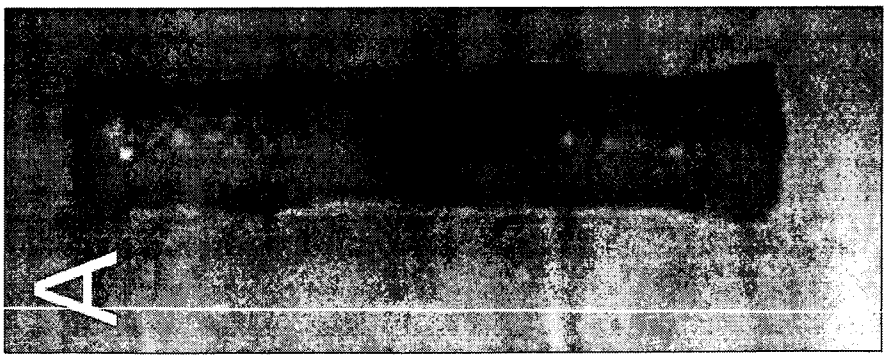

Figure 7 a

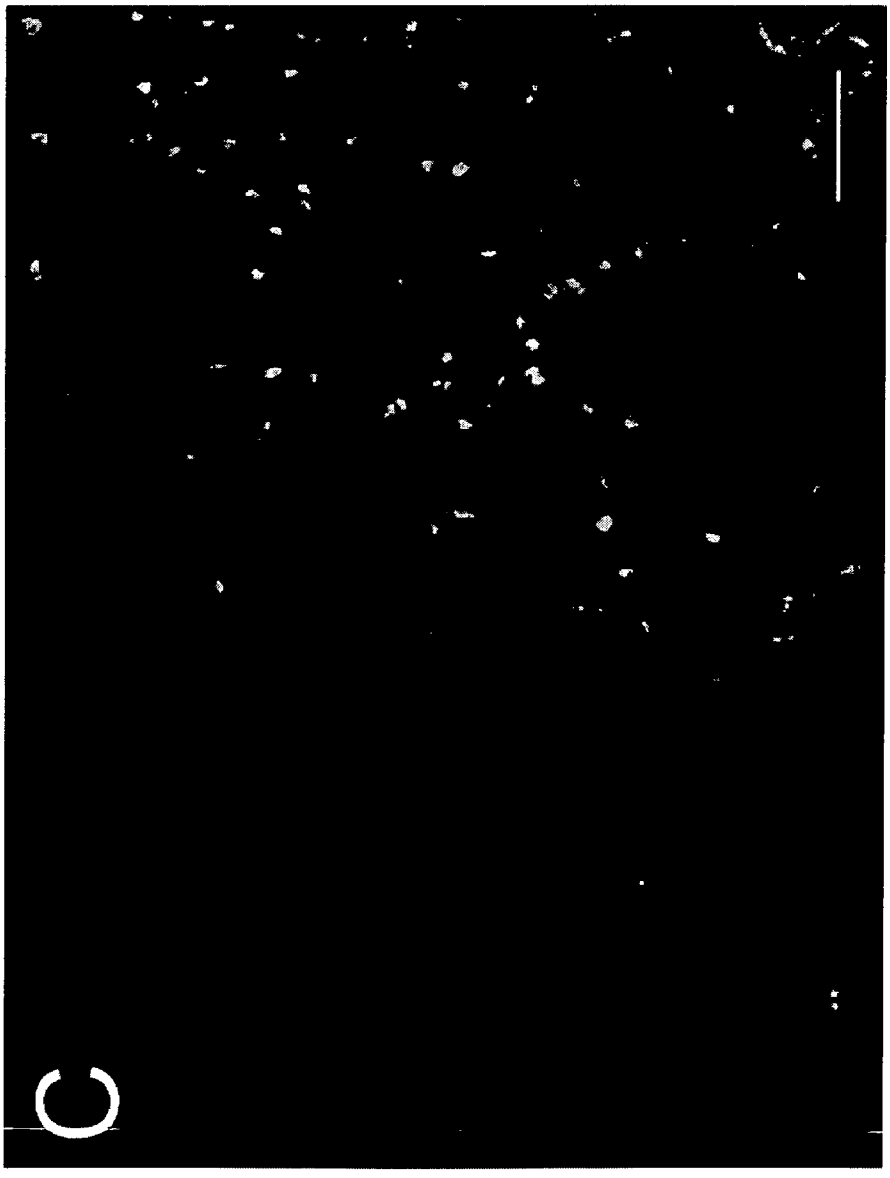

Figure 7 c

Figure 7 d

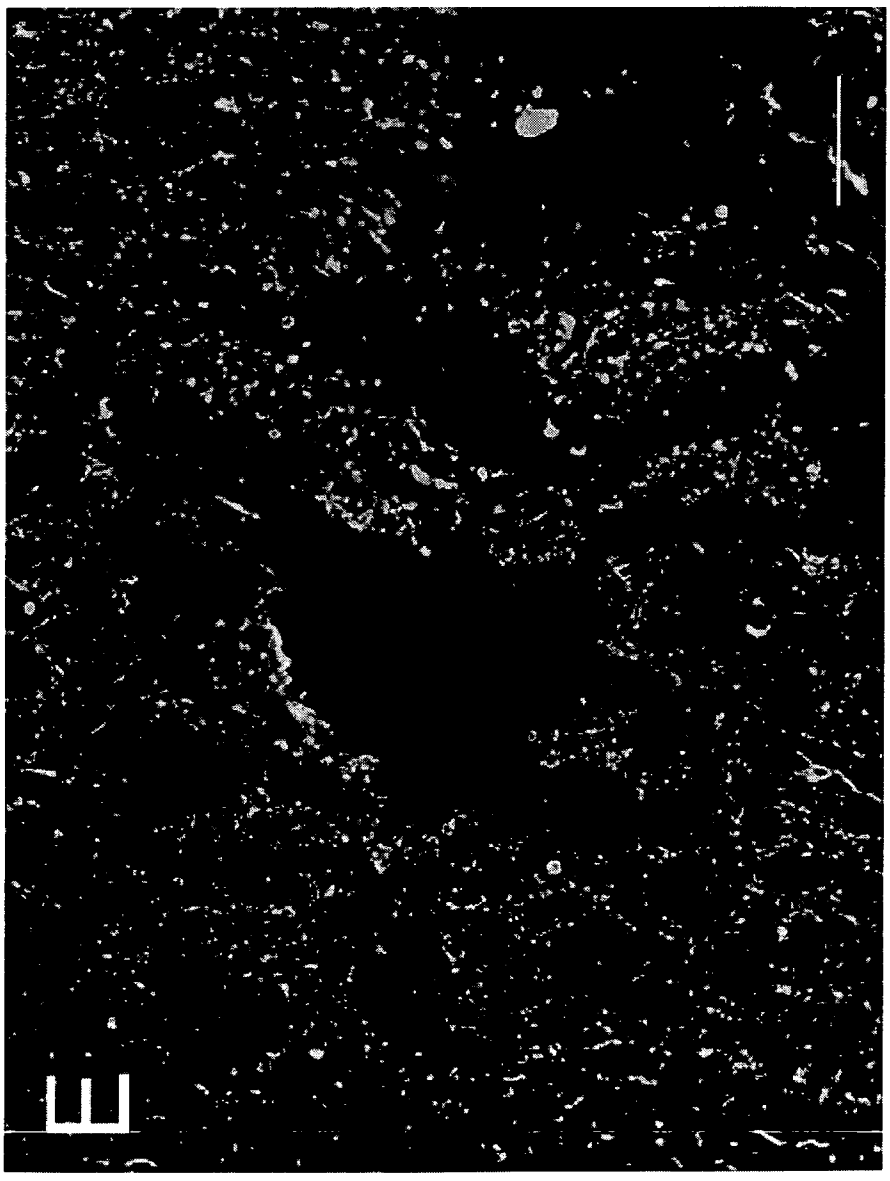

Figure 7 e

Figure 7 g

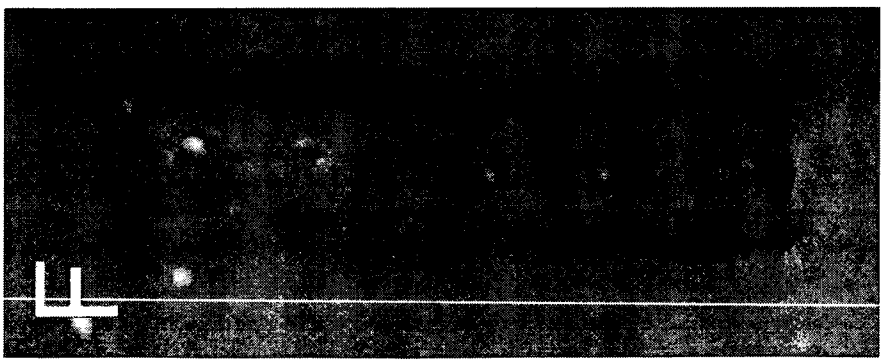

Figure 7 f

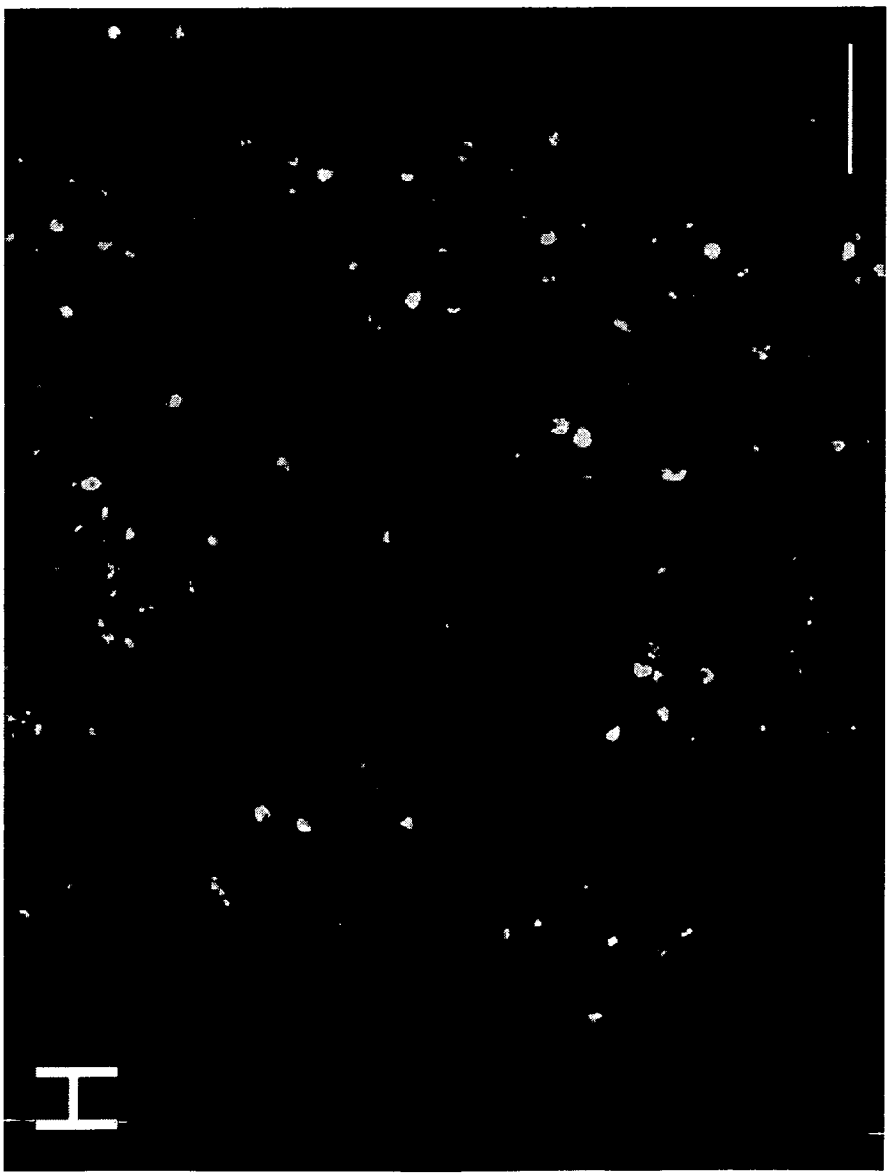

Figure 7 h

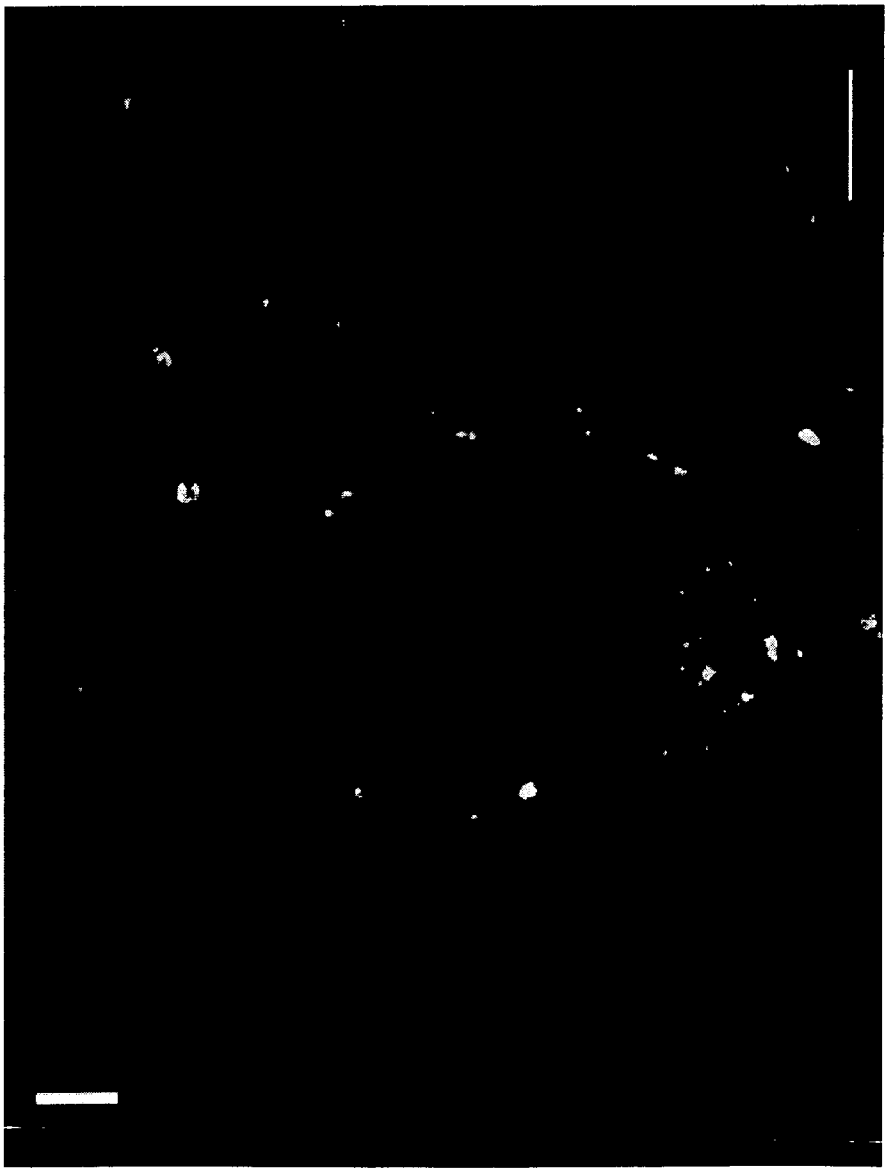

Figure 7 i

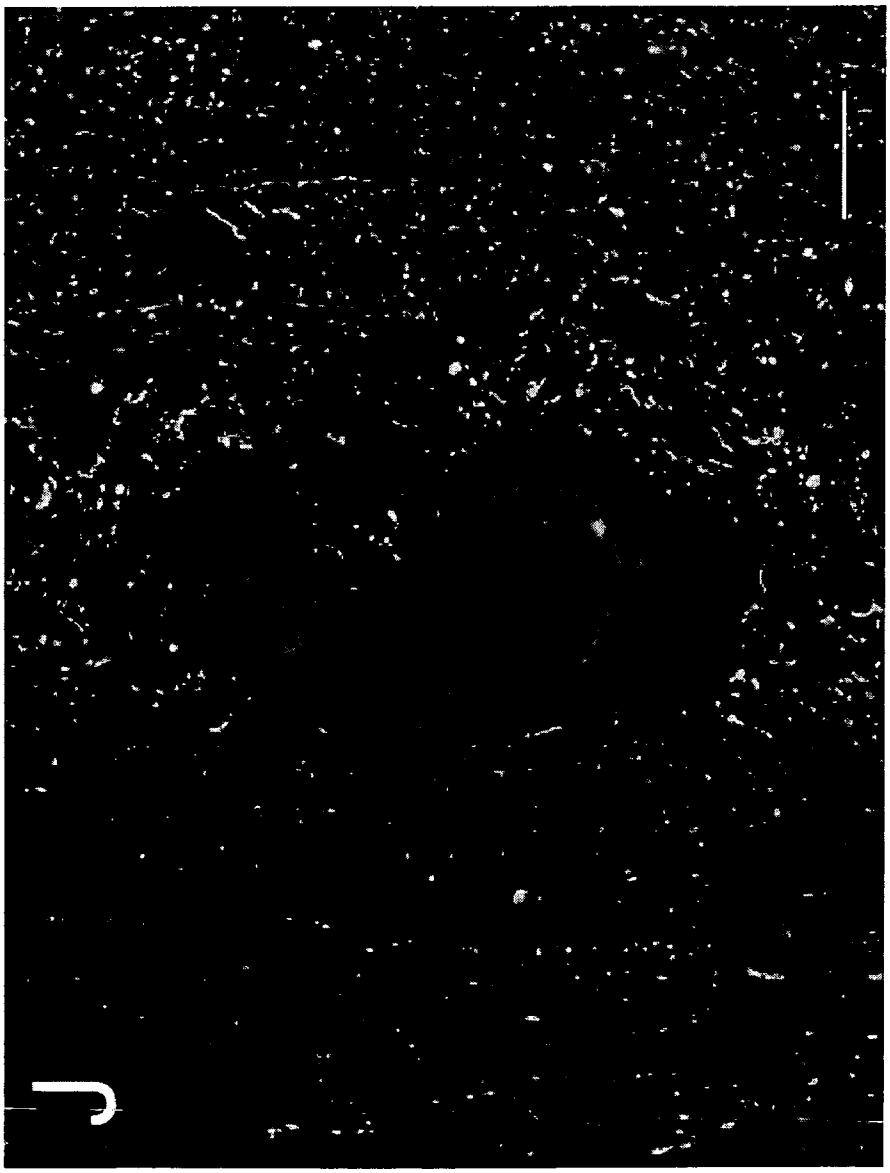

Figure 7 j

Figure 8

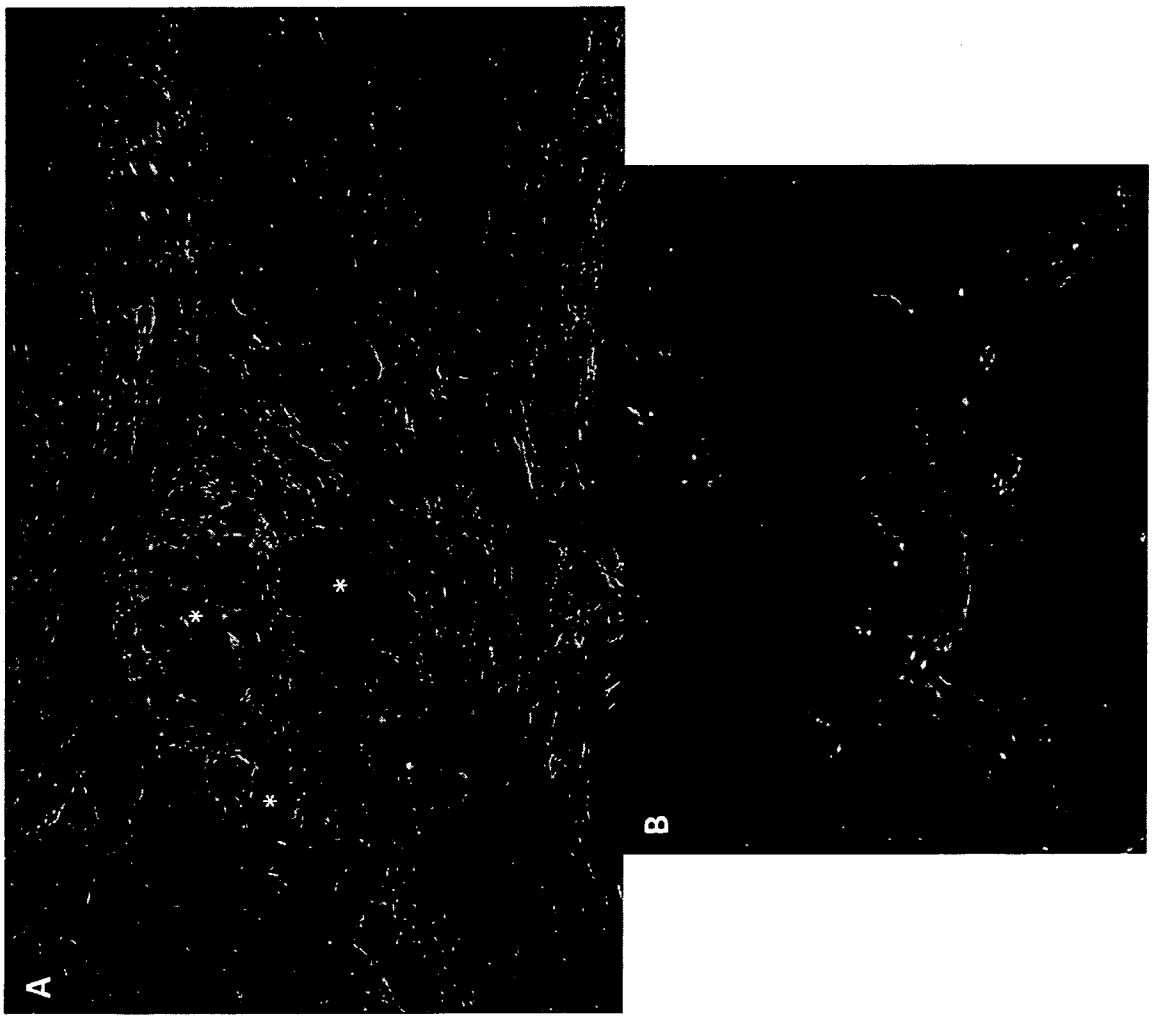

INTERNATIONAL SEARCH REPORT

International application No.
PCT/EP2011/056237

Box No. I Nucleotide and/or amino acid sequence(s) (Continuation of item 1.c of the first sheet)

1. With regard to any nucleotide and/or amino acid sequence disclosed in the international application and necessary to the claimed invention, the international search was carried out on the basis of:

   a. (means)

   - [ ] on paper
   - [X] in electronic form

   b. (time)

   - [X] in the international application as filed
   - [ ] together with the international application in electronic form
   - [ ] subsequently to this Authority for the purpose of search

2. [ ] In addition, in the case that more than one version or copy of a sequence listing and/or table relating thereto has been filed or furnished, the required statements that the information in the subsequent or additional copies is identical to that in the application as filed or does not go beyond the application as filed, as appropriate, were furnished.

3. Additional comments:

INTERNATIONAL SEARCH REPORT

International application No.
PCT/EP2011/056237

Box No. II Observations where certain claims were found unsearchable (Continuation of item 2 of first sheet)

This international search report has not been established in respect of certain claims under Article 17(2)(a) for the following reasons:

1. ☐ Claims Nos.:
because they relate to subject matter not required to be searched by this Authority, namely:

2. ☐ Claims Nos.:
because they relate to parts of the international application that do not comply with the prescribed requirements to such an extent that no meaningful international search can be carried out, specifically:

3. ☐ Claims Nos.:
because they are dependent claims and are not drafted in accordance with the second and third sentences of Rule 6.4(a).

Box No. III Observations where unity of invention is lacking (Continuation of item 3 of first sheet)

This International Searching Authority found multiple inventions in this international application, as follows:

see additional sheet

1. ☐ As all required additional search fees were timely paid by the applicant, this international search report covers all searchable claims.

2. ☐ As all searchable claims could be searched without effort justifying an additional fees, this Authority did not invite payment of additional fees.

3. ☒ As only some of the required additional search fees were timely paid by the applicant, this international search report covers only those claims for which fees were paid, specifically claims Nos.:

1-33(partially)

4. ☐ No required additional search fees were timely paid by the applicant. Consequently, this international search report is restricted to the invention first mentioned in the claims; it is covered by claims Nos.:

Remark on Protest

☒ The additional search fees were accompanied by the applicant's protest and, where applicable, the payment of a protest fee.

☐ The additional search fees were accompanied by the applicant's protest but the applicable protest fee was not paid within the time limit specified in the invitation.

☐ No protest accompanied the payment of additional search fees.

INTERNATIONAL SEARCH REPORT

International application No
PCT/EP2011/056237

A. CLASSIFICATION OF SUBJECT MATTER
INV. A61K47/48 C07K14/78 C12N5/00 C07K14/00 B82Y5/00
ADD.

According to International Patent Classification (IPC) or to both national classification and IPC

B. FIELDS SEARCHED

Minimum documentation searched (classification system followed by classification symbols)
A61K C07K C12N

Documentation searched other than minimum documentation to the extent that such documents are included in the fields searched

Electronic data base consulted during the international search (name of data base and, where practical, search terms used)
EPO-Internal, BIOSIS, Sequence Search, EMBASE, WPI Data

C. DOCUMENTS CONSIDERED TO BE RELEVANT

Category*	Citation of document, with indication, where appropriate, of the relevant passages	Relevant to claim No.
X	WO 2008/039483 A2 (MASSACHUSETTS INST TECHNOLOGY [US]; HORII AKIHIRO [US]; ZHANG SHUGUANG) 3 April 2008 (2008-04-03) page 55; tables 2a,b	1-33
X	GELAIN FABRIZIO ET AL: "Designer self-assembling Peptide nanofiber scaffolds for adult mouse neural stem cell 3-dimensional cultures", PLOS ONE 2006,, vol. 1, E119, 1 January 2006 (2006-01-01), pages 1-11, XP002489970, abstract page 6 - page 9; figure 2; table 1	1-33

-/--

[X] Further documents are listed in the continuation of Box C.

[X] See patent family annex.

* Special categories of cited documents :

"A" document defining the general state of the art which is not considered to be of particular relevance

"E" earlier document but published on or after the international filing date

"L" document which may throw doubts on priority claim(s) or which is cited to establish the publication date of another citation or other special reason (as specified)

"O" document referring to an oral disclosure, use, exhibition or other means

"P" document published prior to the international filing date but later than the priority date claimed

"T" later document published after the international filing date or priority date and not in conflict with the application but cited to understand the principle or theory underlying the invention

"X" document of particular relevance; the claimed invention cannot be considered novel or cannot be considered to involve an inventive step when the document is taken alone

"Y" document of particular relevance; the claimed invention cannot be considered to involve an inventive step when the document is combined with one or more other such documents, such combination being obvious to a person skilled in the art.

"&" document member of the same patent family

Date of the actual completion of the international search	Date of mailing of the international search report
6 October 2011	13/10/2011

Name and mailing address of the ISA/	Authorized officer
European Patent Office, P.B. 5818 Patentlaan 2 NL - 2280 HV Rijswijk Tel. (+31-70) 340-2040, Fax: (+31-70) 340-3016	Vollbach, Silke

4

Form PCT/ISA/210 (second sheet) (April 2005)

C(Continuation). DOCUMENTS CONSIDERED TO BE RELEVANT

Category*	Citation of document, with indication, where appropriate, of the relevant passages	Relevant to claim No.
X	HUCKNALL A M: "A Self-Assembling Peptide Scaffold Functionalized for Use with Neural Stem Cells", 22 July 2005 (2005-07-22), 20050722, XP002489971, the whole document -----	1-33
X,P	GELAIN FABRIZIO ET AL: "BMHP1-derived self-assembling peptides: hierarchically assembled structures with self-healing propensity and potential for tissue engineering applications.", ACS NANO 22 MAR 2011 LNKD-PUBMED:21314189, vol. 5, no. 3, 22 March 2011 (2011-03-22), pages 1845-1859, XP000002658201, ISSN: 1936-086X table 1 -----	1-33

INTERNATIONAL SEARCH REPORT

Information on patent family members

International application No
PCT/EP2011/056237

Patent document cited in search report	Publication date	Patent family member(s)	Publication date
WO 2008039483 A2	03-04-2008	EP 2066697 A2	10-06-2009
		JP 2010504972 A	18-02-2010
		US 2009162437 A1	25-06-2009

FURTHER INFORMATION CONTINUED FROM PCT/ISA/ 210

This International Searching Authority found multiple (groups of) inventions in this international application, as follows:

1. claims: 1-33(partially)

A self-assembling peptide according to SEQ ID No. 1 and uses thereof

---

2-47. claims: 1-33(partially)

A self-assembling peptide according to SEQ ID Nos. 2 to 47 respectively and uses thereof

---